No. 1C-c66 PLZT

1a	Transparency of hot-pressed PLZT ceramics was reported by Haertling in 1971.	71Hae1
b	PLZT means La-modified $Pb(Zr,Ti)O_3$ ceramics. The specimen is often prepared according to the general formula $(Pb_{1-x}La_x)(Zr_yTi_{1-y})_{1-x/4}O_3$ [= $(1-x)Pb(Zr_yTi_{1-y})O_3 \cdot x\ La(Zr_yTi_{1-y})_{3/4}O_3$]. The true composition, however, seems to be intermediate between the above one and $(Pb_{1-x'}La_{2x'/3})(Zr_yTi_{1-y})O_3$ [= $(1-x')Pb(Zr_yTi_{1-y})O_3 \cdot x'\ La_{2/3}(Zr_yTi_{1-y})\ O_3$], where x' = 3x/2. Compositions are ordinarily specified by X/Y/Z, where X = 100x, Y = 100y and Z = 100(1−y). Phase diagram: Figs. 1C-c66-001...1C-c66-004; see also Transition temperature: Figs. 1C-c66-005...1C-c66-007; see also	81Gal 72Kra, 74Wol
2a	Preparation of transparent ceramics: hot-pressing technique atmosphere sintering	71Hae1 73Sno
3a	Lattice parameter: Table 1C-c66-001; Fig. 1C-c66-008, Fig. 1C-c66-009. See also For impurity effect: see	74Wol 81Har
4	Thermal expansion: Fig. 1C-c66-010, Fig. 1C-c66-011.	
5a	Dielectric constant: Figs. 1C-c66-012...1C-c66-034; see also	74Wol, 75Wol
	For additional data: see	80Gur, 80Ste1, 83Yao, 84Ish, 86Yok
	Field effect: Fig. 1C-c66-035. Effect of hydrostatic pressure: Fig. 1C-c66-036.	
c	Polarization and coercive field: Figs. 1C-c66-037...1C-c66-045. For additional data: see	79Lan, 80Ste2, 81Sch, 83Yao, 86Woj
d	Pyroelectricity: see Table 1C-c66-002, and also	74Liu
6a	Heat capacity: Fig. 1C-c66-046, Fig. 1C-c66-047. Transition enthalpy: see Thermal conductivity: Fig. 1C-c66-048.	80Ste3
7a	Electromechanical properties: Table 1C-c66-002; Fig.1C-c66-049; see also	71Hae1, 72Mei
	Piezoelectricity: Fig. 1C-c66-050. Compositional dependence: see	85Uch, 85Smi
b	Electrostriction: Table 1C-c66-003; see also	85Men
8a	Ultrasonic velocity: Fig. 1C-c66-051. Elastic constants: Fig. 1C-c66-052, Fig. 1C-c66-053. Elastic compliance: Fig. 1C-c66-054, Fig. 1C-c66-055; see also	85Smi

9a	Refractive index: Table 1C-c66-004, Table 1C-c66-005; Fig. 1C-c66-056. Infrared reflectivity: Fig. 1C-c66-057. Transmission: Fig. 1C-c66-058, Fig. 1C-c66-059; see also Birefringence: Figs. 1C-c66-060...1C-c66-063; see also Absorption: Fig. 1C-c66-064; see also Photorefractive properties: Effect of ion-implantation was studied.	 74Lan, 76Oka 80Fog, 84Cor, 86Kni 82Spr, 84Sea 82Lan, 83Lan, 85Lan
b	Electrooptic effect: Table 1C-c66-006, Table 1C-c66-007; Fig. 1C-c66-065, Fig. 1C-c66-066. Electrooptic effect: Effective quadratic electrooptic constant; $\bar{L}^{\mathrm{T}} = 4.3\cdot 10^{-16}\,\mathrm{m^2V^{-2}}$, $\bar{L}^{\mathrm{S}} = 1.5\cdot 10^{-16}\,\mathrm{m^2V^{-2}}$ at 632.8 nm for PLZT(9/65/35). Fig. 1C-c66-067; see also Light scattering induced by electric field: Fig. 1C-c66-068; see also	 81Kir 81Ste 79Lan
c	Piezooptic effect: Fig. 1C-c66-069, Fig. 1C-c66-070.	
e	Nonlinear optical properties: Fig. 1C-c66-071, Fig. 1C-c66-072; see also Fig. 1C-c66-073; see	 81Lib
10a	Raman scattering: Table 1C-c66-008; see also	74Lur
11	Electrical conduction: Figs. 1C-c66-074...1C-c66-076; see also	82Spr, 86Woj
12	Effect of magnetic field on dielectric constant: see Fig. 1C-c66-020 in 5a.	
15a	Domain structure: see	94Zha, 93DeG, 75Kev, 77Miy, 92Pla
16	Thin films were sputtered on various substrates: see Thin film growth: RF sputtering: see MOCVD: see Laser ablation: see Ion beam sputtering: see Electrophoretic deposition: see Sol-gel method: see Dielectric constant for thin films: Fig. 1C-c66-077, Fig. 1C-c66-078.	77Mat, 78Mat, 78Hig 79Nak, 80Oku, 80Mat 92Oka, 93Tom, 94Tom 90Pet, 92Pet 90Boy, 92Tos 91Sug 94YeC

Table 1C-c66-001. PLZT. Lattice parameters [71Hae1].

Composition (La/Zr/Ti)	Phase	a [Å]	c [Å]	$\sqrt[3]{V}$ [Å]	V [$Å^3$]	ρ_{theor} [$\cdot 10^3$ kgm^{-3}]
2/65/35	rh			4.093	68.57	7.976
6/65/35	rh			4.092	68.52	7.900
8/65/35	rh			4.091	68.47	7.863
9/65/35				4.091	68.47	7.845
10/65/35				4.091	68.47	7.824
12/65/35				4.090	68.42	7.784
8/80/20	tetr/cub			4.116	69.73	7.872
8/70/30	rh			4.088	68.32	7.932
8/65/35	rh			4.091	68.47	7.863
8/60/40	tetr/rh	4.078	4.086		67.95	7.871
8/58/42	tetr	4.076	4.088		67.92	7.854
8/53/47	tetr	4.051	4.081		66.97	7.912
8/50/50	tetr	4.059	4.086		67.32	7.892
8/40/60	tetr	4.029	4.074		66.13	7.874
8/10/90	tetr	3.971	4.034		63.61	7.854
7/65/35	rh			4.096	68.72	7.856
7/62/38	rh			4.086	68.22	7.882
7/58/42	tetr	4.066	4.086		67.55	7.897
4/100/0	mixed	(4.16)	(4.12)		(71.30)	
20/100/0	mixed	(4.16)	(4.14)		(71.65)	
17/90/10	mixed			(4.129)	(70.39)	
18/10/90	tetr	3.958	3.985		62.43	7.787
30/0/100	cub			3.944	61.35	7.551

Note: Values in parentheses are for major $PbZrO_3$ phase.

Table 1C-c66-002. PLZT. Dielectric, piezoelectric and pyroelectric characteristics [74Luf].

Composition			ρ	κ		k_p	d	g	F.M.$_{R_I}$	F.M.$_{R_V}$	p
X	Y	Z	[$\cdot 10^3$ kg m^{-3}]	unpoled	poled		[$\cdot 10^{-12}$ C N^{-1}]	[$\cdot 10^{-3}$ m^2 C^{-1}]	[$\cdot 10^{-11}$ C m J^{-1}]	[$\cdot 10^{-13}$ C m J^{-1}]	[$\cdot 10^{-4}$ C m^{-2} K^{-1}]
6.7	76	24	7.70	2400	1360	0.34	288	24	22	17	6.0
7.3	76	24	7.68	2680	3050	0.13	233	9	12	4.5	2.8
7.9	76	24	7.62	2800	3280	<0.1	57	2	4.1	1.4	0.72
8.5	76	24	7.61	2600	3280	<0.1	10	0.4	1.3	0.5	0.27
7.7	72	28	7.63	3300	2860	0.40	525	21	30	12	10.0
8.3	72	28	7.61	3210	3420	<0.1	38	1.2	0.81	0.25	0.24
8.2	68	32	7.61	3690	4390	0.43	500	13	40	12	3.6
9.0	68	32	7.59	3850	4160	<0.1			1.3	0.33	0.44
7.7	64	36	7.68	3020	2970	0.54	700	27	26	10	6.7
8.1	64	36	7.65	3770	3670	0.55	700	22	31	9.5	10.9
8.5	64	36	7.60	4220	4840	0.31	565	14	24	6.3	8.8
5.7	60	40	7.76	1570	1370	0.46	360	30	14	11	3.4
6.1	60	40	7.75	1750	1600	0.51	440	31	17	11	4.4
6.5	60	40	7.75	2000	3210	0.52	550	28	18	8.7	4.7
2.6	56	44	7.54	1070	970	0.42	330	39	12	12	2.7
3.0	56	44	7.36	1060	1060	0.45	380	42	13	12	2.9
3.4	56	44	7.36	1150	1080	0.46	390	40	13	12	3.1

F.M.$_{R_I}$: Figure of merit for current responsivity.
F.M.$_{R_V}$: Figure of merit for voltage responsivity.
k_p: electromechanical coupling factor.

Table 1C-c66-003. PLZT (ceramics). Electrostrictive constants at room temperature [85Men].

Composition	Q_{11} [$\cdot 10^{-3}$ m^{4}C^{-2}]	Q_{21} [$\cdot 10^{-3}$ m^{4}C^{-2}]
7/65/35	22.5	–11.5
7.5/65/35	16.3	–8.7
8/65/35	18.3	–8.1
8.8/65/35	21.2	–9.5
9.5/65/35	21.0	–9.1
8/70/30	9.7	–7.5

Table 1C-c66-004. PLZT. Refractive indices *n* vs. *λ* [77Tha].

λ	Composition									
[nm]	8/100/0 [a])	8/90/10	8/80/20	10/65/35	2/65/35	16/40/60	16/20/80	24/10/90	8/10/90	0/0/100 [b])
405	2.62		2.697	2.714		2.811				
436	2.56	2.586	2.635	2.648	2.697	2.734	≈2.82	2.846	2.860	
492	2.50	2.520	2.563	2.576		2.645	2.723		2.757	2.781
546	2.46	2.481	2.520	2.532	2.570	2.600	2.667	2.687	2.700	2.725
579	2.44	2.463	2.502	2.513	2.549	2.579	2.644		2.675	2.699
633	2.42	2.441	2.479	2.490	2.523	2.552	2.613	2.631	2.644	2.668
680	2.41	2.427					2.594		2.623	2.646
710	2.40	2.420	2.455	2.466		2.525				2.636
764	2.39		2.444	2.455		2.514				2.619

[a]) Extrapolated values as y tend to zero in the $[Pb_{0.92}\,La_{0.08}]\,[Zr_y\,Ti_{1-y}]_{0.98}O_3$ system.
[b]) Calculated values as$(2n_o+n_e)/3$, using parameters for the Sellmeier equation reported in [72Sin].

Table 1C-c66-005. PLZT (10/65/35). Refractive indices vs. λ [77Tha].

λ [μm]	n	λ [μm]	n
0.901	2.433	1.760	2.388
0.950	2.428	2.145	2.379
1.000	2.423	2.424	2.373
1.155	2.412	2.580	2.371
1.375	2.401		

Table 1C-c66-006. PLZT, PLHT, and PBLN. Electrooptic constant [81Kir]. $r'_c = (n_c/n_a)^3 r^T_{33} - r^T_{13}$. For specifications of compositions, see subsection 1b of substance No. 1C-c66 and No. 1C-c64 (except PBLN).

Composition		r'_c [$\cdot 10^{-10}$ m V^{-1}]	Ref.
PLZT	14/30/70	1.12 (λ = 633 nm)	71Hae1
	8/40/60	1.02	
	7/62/38	4.43	
	8/65/35 (10 μm) [a]	5.23	
	8/65/35 (3 μm) [a]	6.12	
	12/40/60	1.4 (λ = 546 nm)	72Tha
PLHT	8/40/60 (1.5 μm) [a]	1.68 (λ = 633 nm)	73Cut
	8/40/60 (3.0 μm) [a]	1.52	
PBLN [b]	3/60/40	7.45 (λ = 633 nm)	77Yok
	4/60/40	6.66	

[a]) Grain size.
[b]) $(Pb_{1-y}Ba_y)_{1-x}La_xNb_{2-x/5}O_6$. Compositions are specified by 100x/(100(1 − y)/100y.

Table 1C-c66-007. PLZT, PLHT, and PBLN. Quadratic electrooptic constant [81Kir]. For specifications of compositions, see subsection 1b of substance No. 1C–c66 and No. 1C–c64 (except PBLN).

Composition		$L_{33} - L_{13}$ [$\cdot 10^{-16}$ m^2 V^{-2}]	$M_{33} - M_{13}$ [m^4 C^{-2}]	Ref.
PLZT	9/65/35	9.116 (λ = 633 nm)	0.018 (λ = 633 nm)	71Hae1
	10/65/35	1.073	0.010	
	11/65/35	0.602	0.014	
	7.5/62/38		0.0113	76Bye
	7.95/70/30		0.0166	
	7.5/72/28		0.0202	
PLHT	9/65/35 (1.8 µm) [b])	2.60		73Cut
	10/65/35 (2.3 µm) [b])	1.80		
PBLN [a])	8/60/40	2.09 (λ = 633 nm)		77Yok
	10/60/40	1.16		

[a]) $(Pb_{1-y}Ba_y)_{1-x}La_xNb_{2-x/5}O_6$. Compositions are specified by 100x/100(1 – y)/100y.
[b]) Grain size.

Table 1C-c66-008. PLZT. Raman frequency shift and optical-phonon assignment [71Bry].

Phonon mode symmetry	Phonon wave number $\Delta\nu/c$ [cm^{-1}]		
	Sample compositions		
	8/10/90	18/10/90	12/40/60
1E(TO)	65		
$1A_1$(TO)	85		
1E(LO)	135	≈135	≈135
$1A_1$(LO)	≈195	≈190	210
2E(TO)	195	190	195
$2A_1$(TO)	330	≈300	320
2E(LO)	445	440	≈430
$2A_1$(LO)	≈495	≈495	≈500
B_1 } 3E(TO) } 3E(LO) }	280	275	270
4E(TO)	510	520	525
$4A_1$(TO)	595	565	560
4E(LO)	≈710	715	710
$4A_1$(LO)	≈750	≈740	795

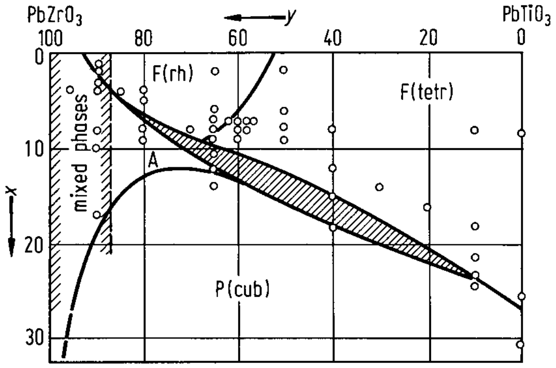

Fig. 1C-c66-001. PLZT. Phase diagram [71Hae1]. Shaded area: not-well-defined broad transition region.

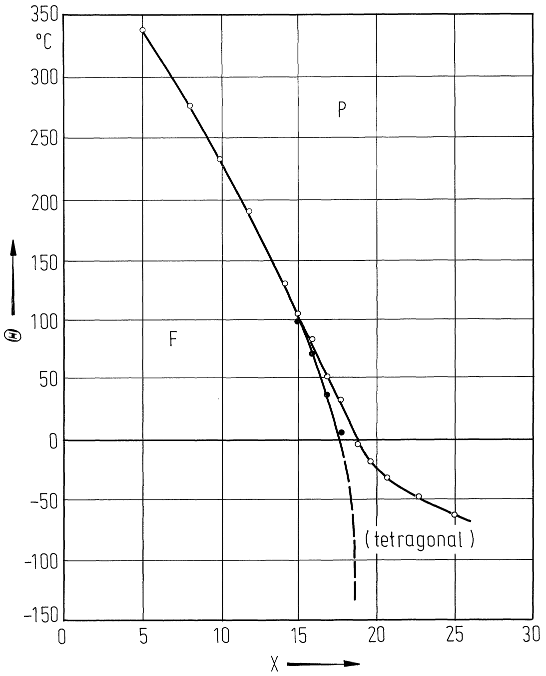

Fig. 1C-c66-002. PLZT(X/30/70). Θ vs. X [80Ste1].

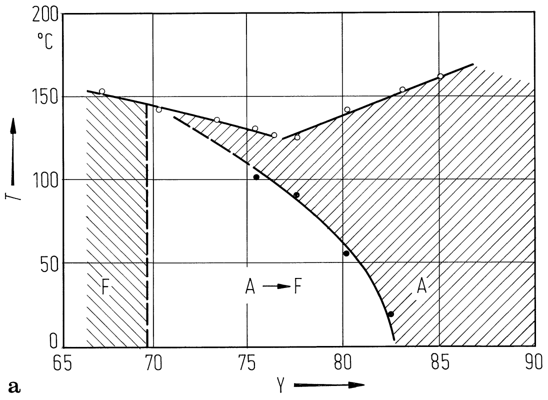

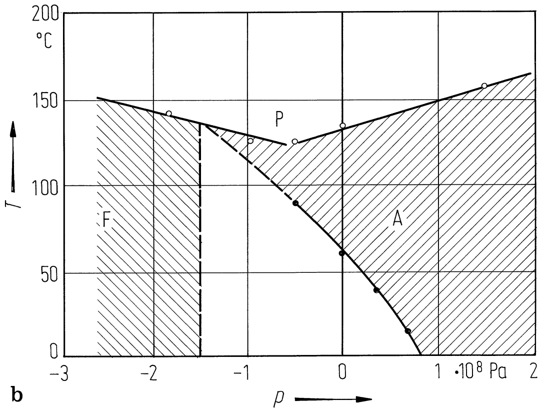

Fig. 1C-c66-003. PLZT. **(a)** *T* vs. Y of PLZT(6/Y/100−Y), **(b)** *T* vs. *p* for PLZT(6/80/20) [81Gal].

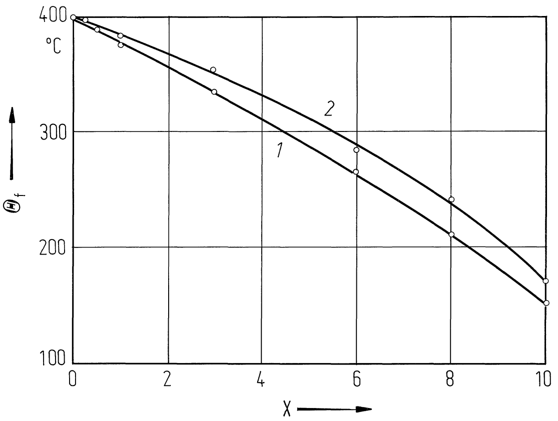

Fig. 1C-c66-004. PLZT(X/52/48) (ceramics). Θ_f vs. X [86Woj]. Curve *1*: on cooling; *2*: on heating.

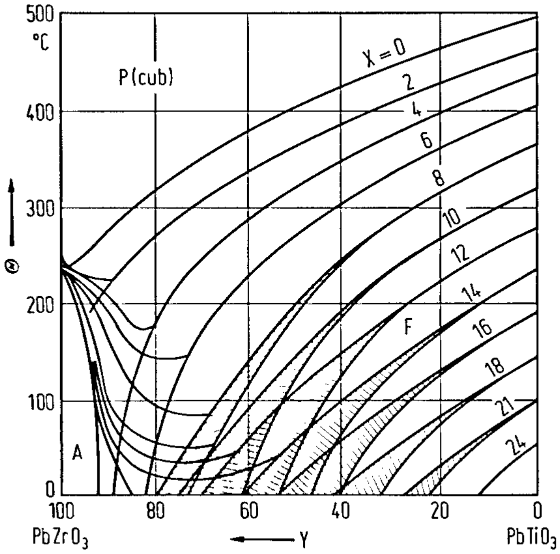

Fig. 1C-c66-005. PLZT. Θ vs. Y [71Hae1]. Parameter: X.

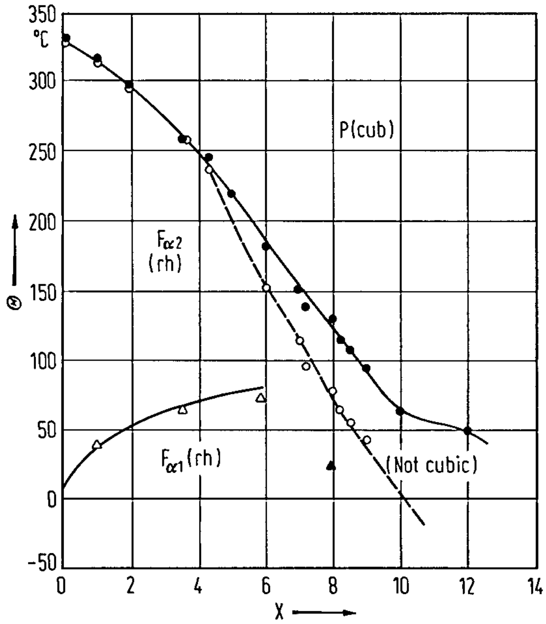

Fig. 1C-c66-006. PLZT(X/65/35). Θ vs. X [73Mei]. Determined for annealed ceramics. Full circles: maximum in κ (f = 120 Hz...10 kHz), open circles: peak in dielectric tan δ, open triangles: minimum in longitudinal sound velocity, full triangle: limit of domain existence observed by chemical etching.

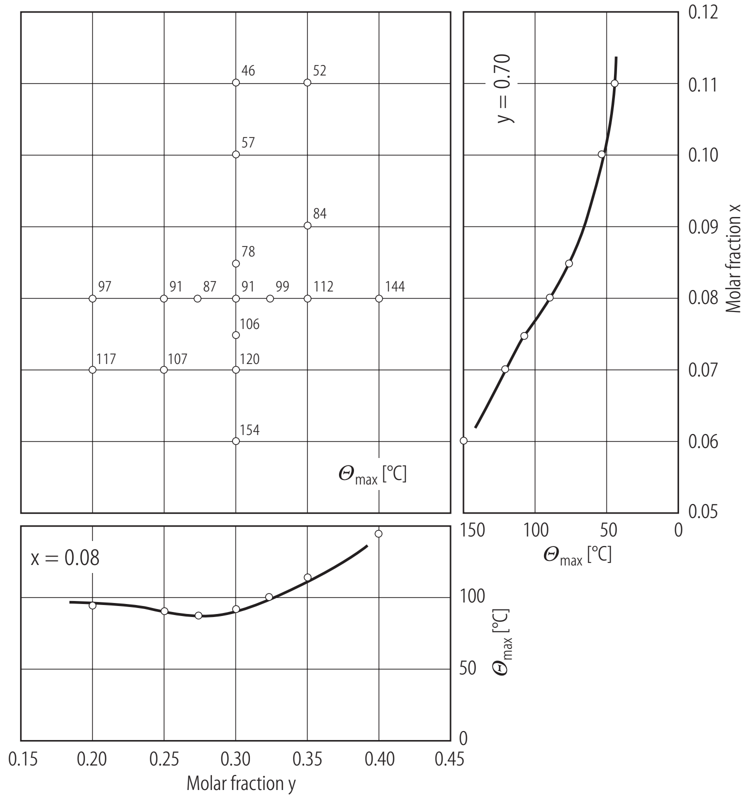

Fig. 1C-c66-007. $(Pb_{1-x}La_x)(Zr_{1-y}Ti_y)_{1-x/4}O_4$ (PLZT 100x/100y/100(1−y)) (ceramics). Θ_{max} vs. x, y [91Ohk]. Θ_{max}: temperature of maximum dielectric constant at 10 kHz.

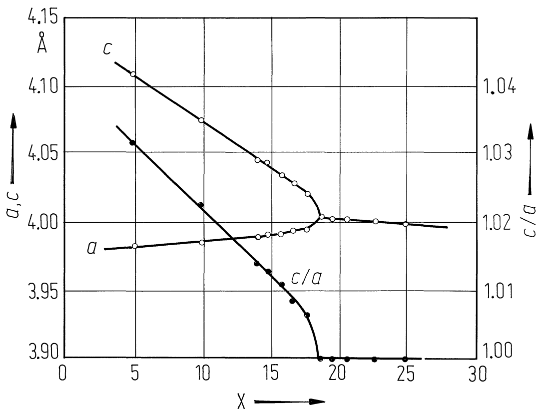

Fig. 1C-c66-008. PLZT(X/30/70). *a*, *c*, *c*/*a* vs. X [80Ste1].

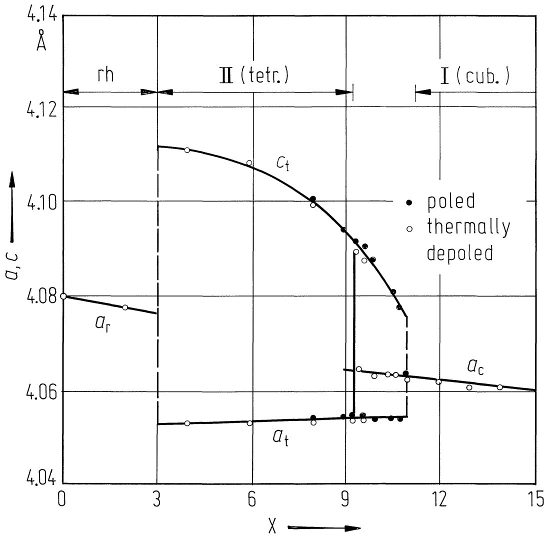

Fig. 1C-c66-009. PLZT(X/55/45). *a*, *c* vs. X [86Yok].

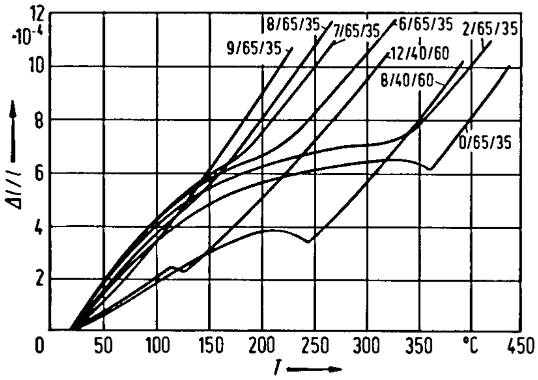

Fig. 1C-c66-010. PLZT. $\Delta l/l$ vs. T [71Hae2]. Parameter: composition.

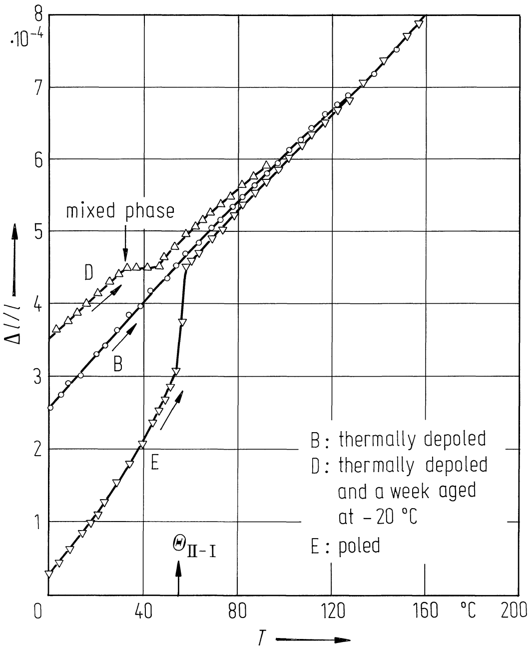

Fig. 1C-c66-011. PLZT(10/55/45) (ceramics). $\Delta l/l$ vs. T [86Yok].

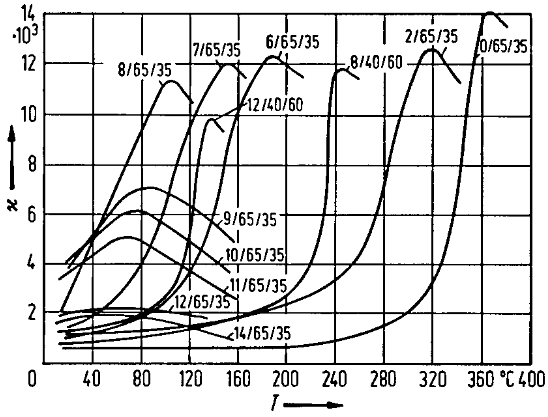

Fig. 1C-c66-012. PLZT. κ vs. T [71Hae1]. Parameter: composition. f = 1 kHz.

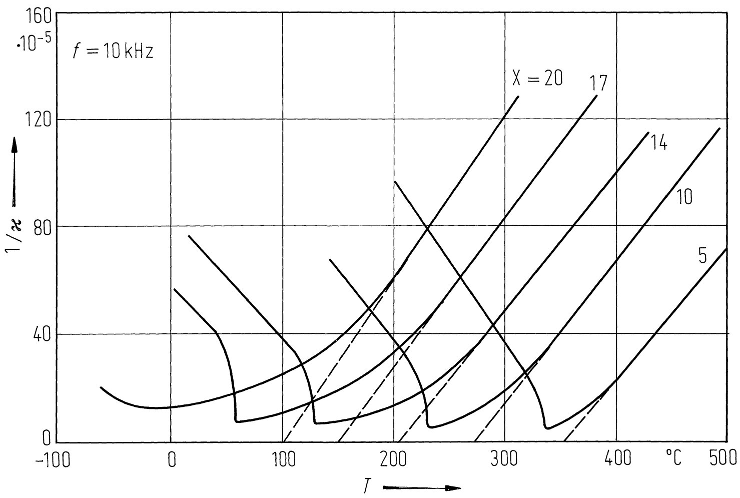

Fig. 1C-c66-013. PLZT(X/30/70) (ceramics). κ^{-1} vs. T [80Ste3]. Parameter: X. f = 10 kHz.

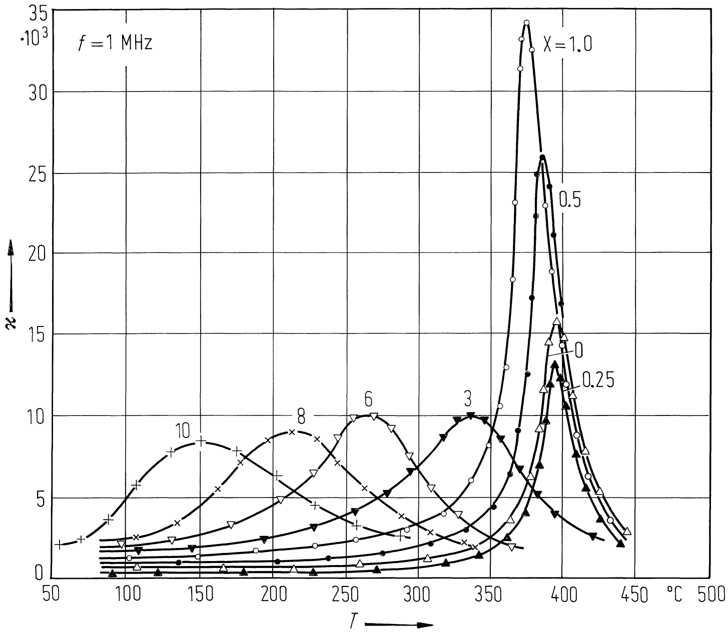

Fig. 1C-c66-014. PLZT(X/52/48) (ceramics). κ vs. T [86Woj]. Parameter: X.

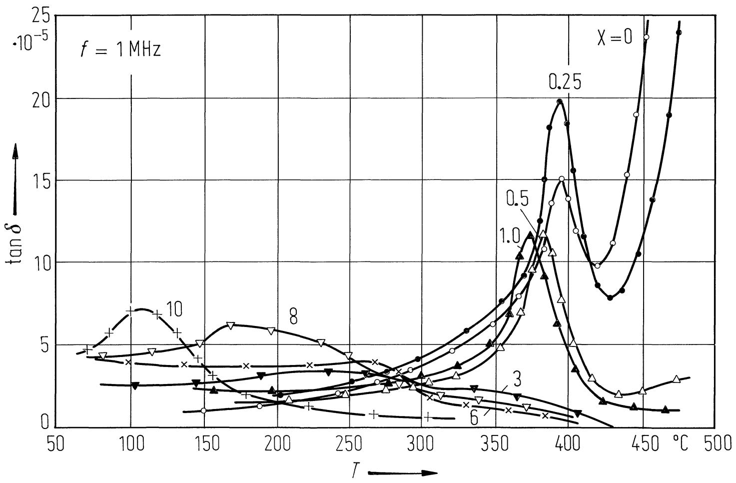

Fig. 1C-c66-015. PLZT(X/52/48) (ceramics). tan δ vs. T [86Woj]. Parameter: X. f = 1MHz.

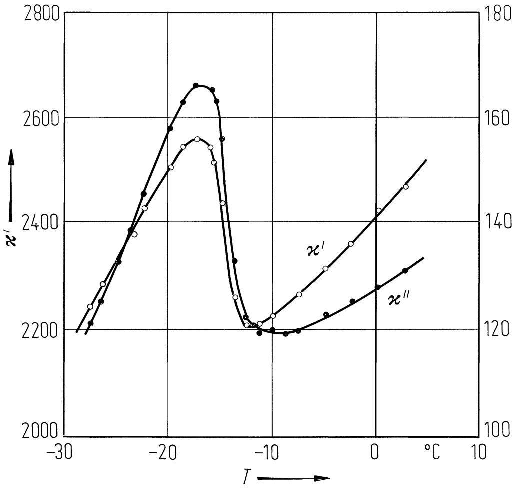

Fig. 1C-c66-016. PLZT(10/65/35) (ceramics). *κ*' , *κ*'' vs. *T* [84Cor].

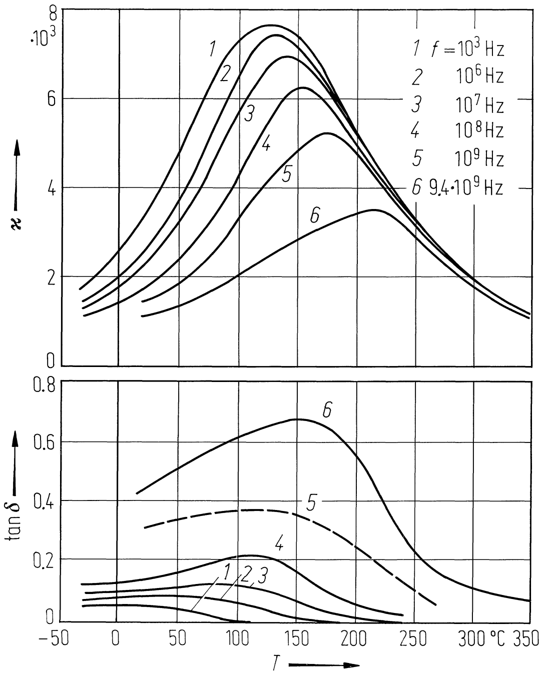

Fig. 1C-c66-017. PLZT(8/65/35) (ceramics). *κ*, tan *δ* vs. *T* [83Ker]. Parameter: *f*.

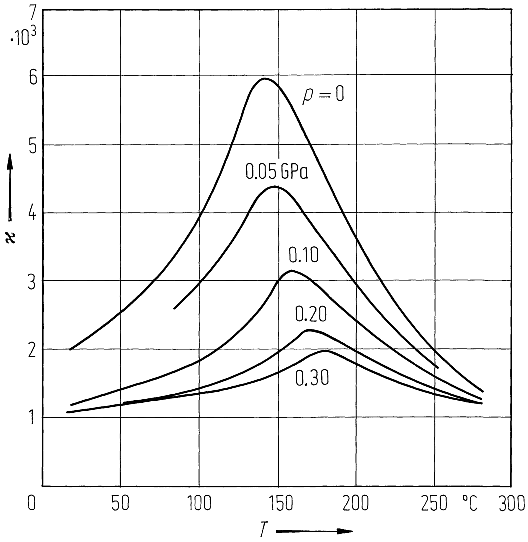

Fig. 1C-c66-018. PLZT(6/80/20) (ceramics). *κ* vs. *T* [84Ish]. Parameter: *p*.

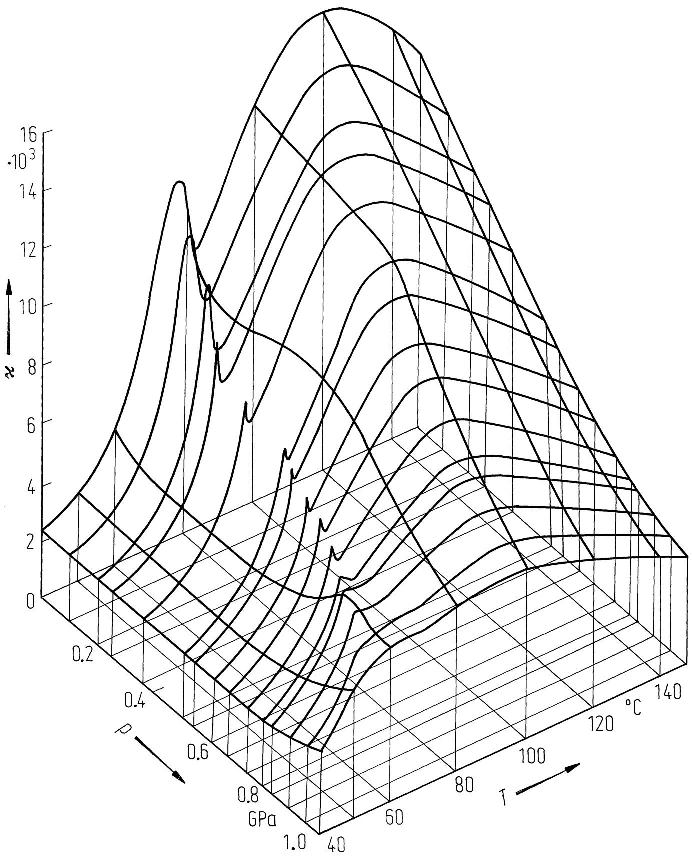

Fig. 1C-c66-019. PLZT(8/65/35) (ceramics). κ vs. p, T [80Fri].

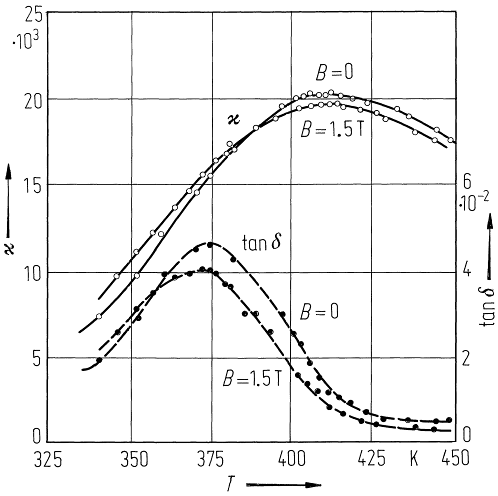

Fig. 1C-c66-020. PLZT(7/65/35) (ceramics). κ, tanδ vs. T [83Ste]. Parameter: B. B: magnetic induction.

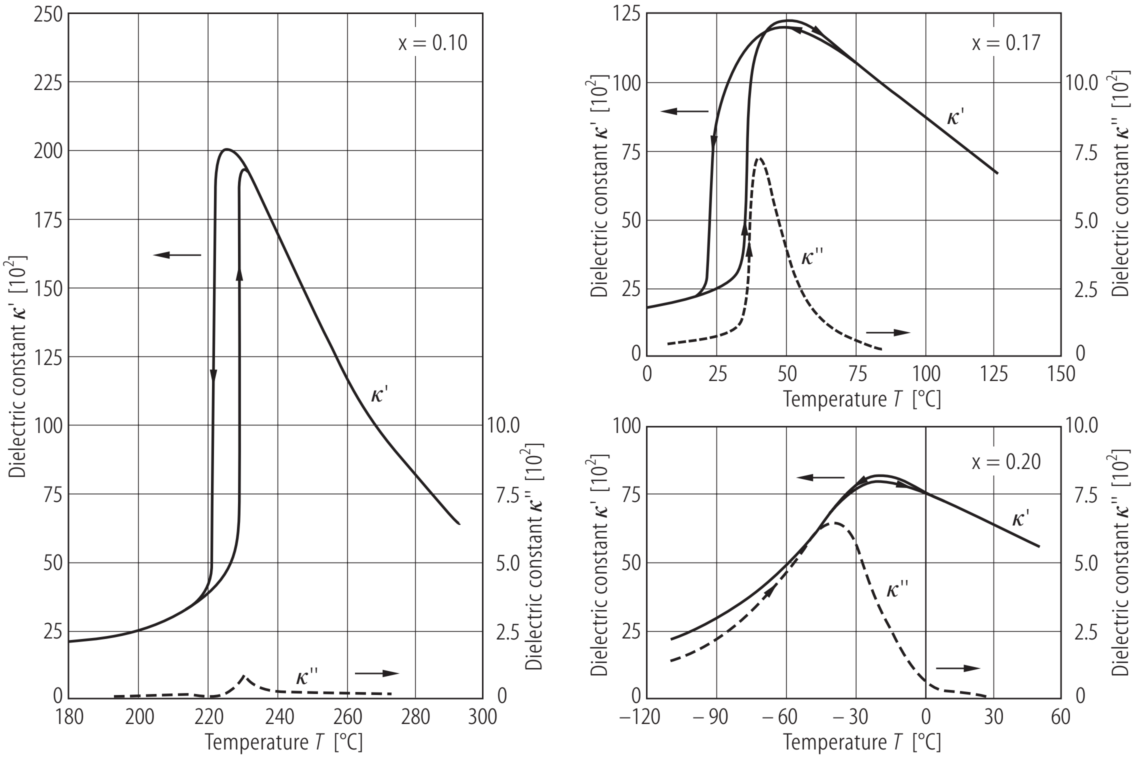

Fig. 1C-c66-021. $(Pb_{1-x}La_x)(Zr_{0.30}Ti_{0.70})_{1-x/4}O_3$ (PLZT 100x/30/70) (ceramics). κ', κ'' vs. *T* [80Ste1].

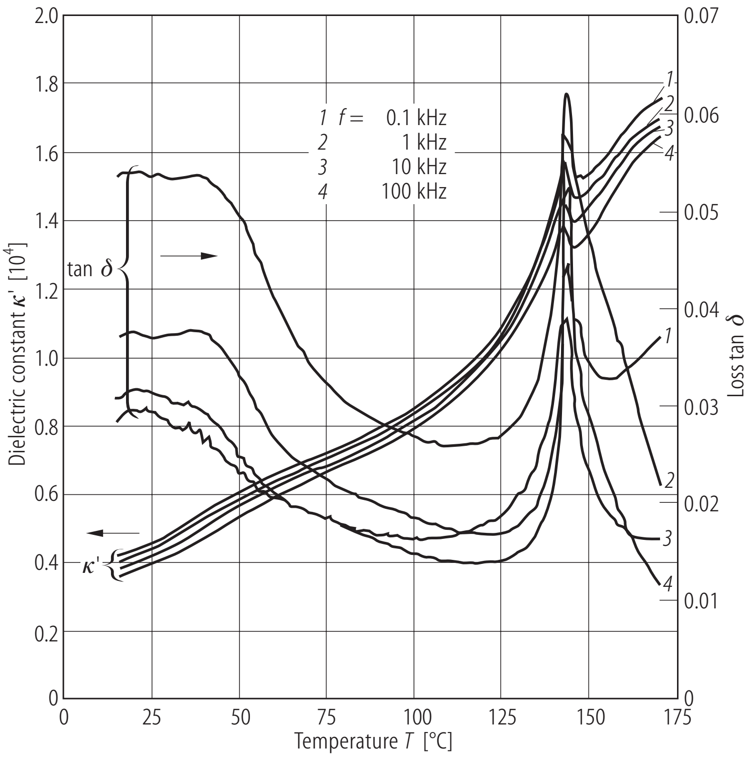

Fig. 1C-c66-022. $(Pb_{0.92}La_{0.08})(Zr_{0.40}Ti_{0.60})_{0.98}O_3$ (PLZT 8/40/60) (ceramics). κ', $\tan\delta$ vs. T [87Deb]. Parameter: f. Details of the data between 0 and 70 °C.

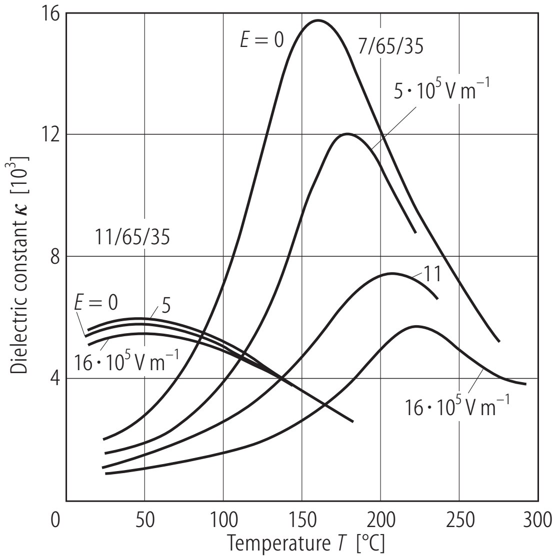

Fig. 1C-c66-023. $(Pb_{1-x}La_x)(Zr_yTi_{1-y})_{1-x/4}O_3$ (PLZT 100x/100y/100(1−y)) (ceramics). κ vs. T [87Nag]. Parameter: E_{bias}.

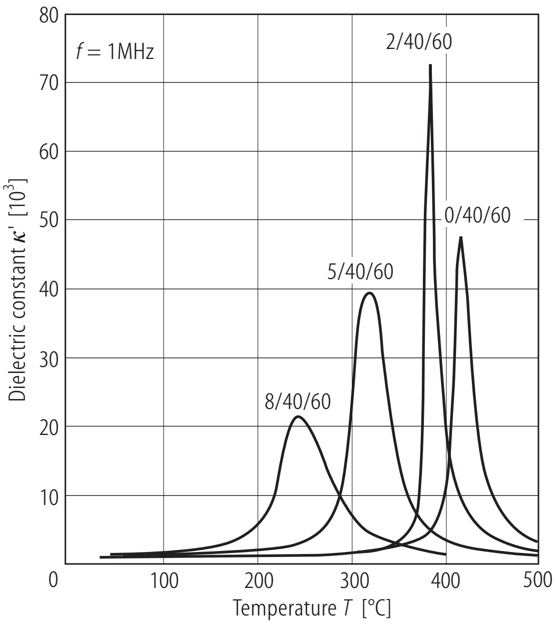

Fig. 1C-c66-024. $(Pb_{1-x}La_x)(Zr_{0.40}Ti_{0.60})_{1-x/4}O_3$ (PLZT 100x/40/60) (ceramics). κ' vs. T [93Dai]. Parameter: x. f = 1 MHz.

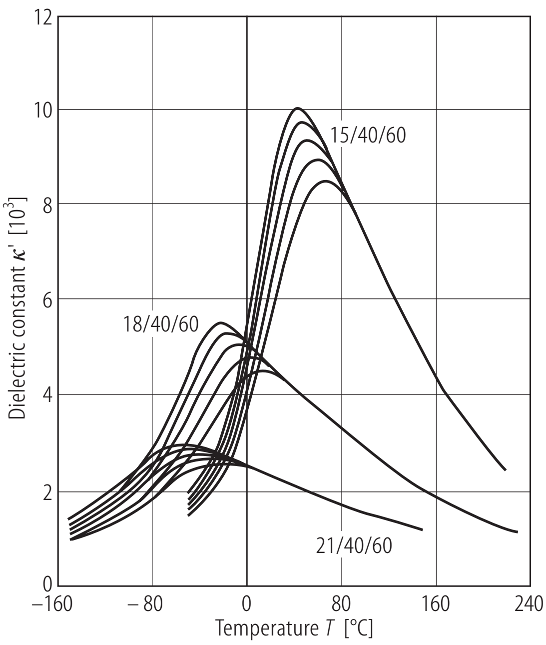

Fig. 1C-c66-025. $(Pb_{1-x}La_x)(Zr_{0.40}Ti_{0.60})_{1-x/4}O_3$ (PLZT 100x/40/60) (ceramics). κ' vs. T [93Dai]. Parameter: x, *f*. f = 100 Hz, 1 kHz, 10 kHz, 100 kHz, 1 MHz from top to bottom curves for each composition.

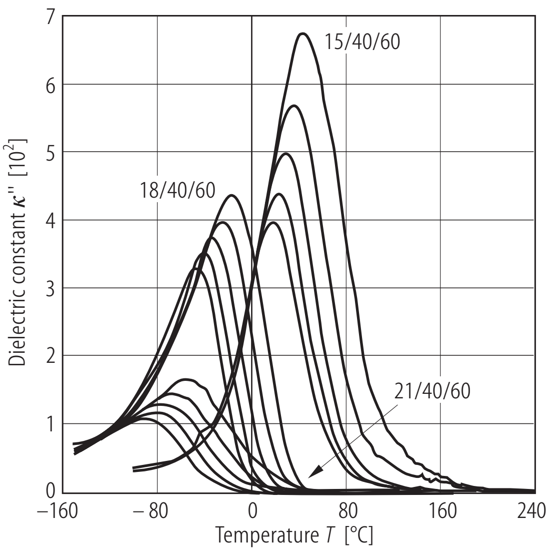

Fig. 1C-c66-026. $(Pb_{1-x}La_x)(Zr_{0.40}Ti_{0.60})_{1-x/4}O_3$ (PLZT 100x/40/60) (ceramics). κ'' vs. T [93Dai]. Parameter: x, *f*. *f* = 100 Hz, 1 kHz, 10 kHz, 100 kHz, 1 MHz from bottom to top curves for each composition.

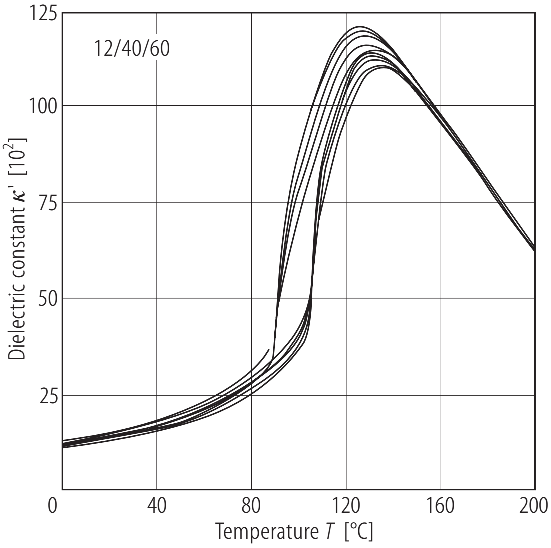

Fig. 1C-c66-027. $(Pb_{0.88}La_{0.12})(Zr_{0.40}Ti_{0.60})_{0.97}O_3$ (PLZT 12/40/60) (ceramics). κ' vs. T on cooling and heating [93Dai]. f = 100 Hz, 1 kHz, 10 kHz, 100 kHz, 1 MHz from top to bottom curves of cooling and heating runs.

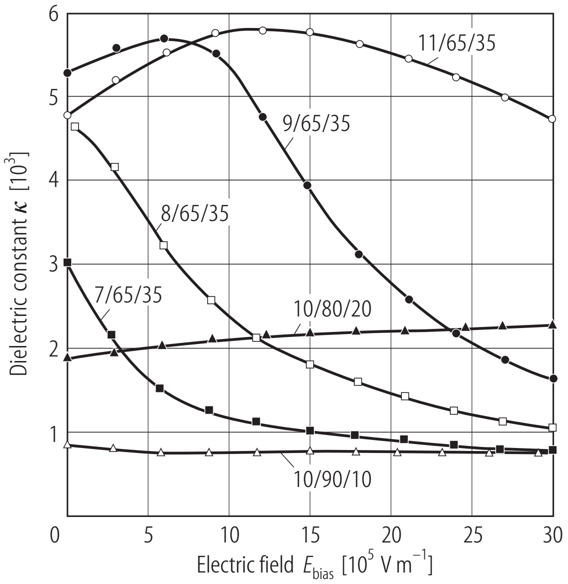

Fig. 1C-c66-028. $(Pb_{1-x}La_x)(Zr_yTi_{1-y})_{1-x/4}O_3$ (PLZT 100x/100y/100(1−y)) (ceramics). κ vs. E_{bias} [90Nag]. Parameter: x, y. f = 1 kHz.

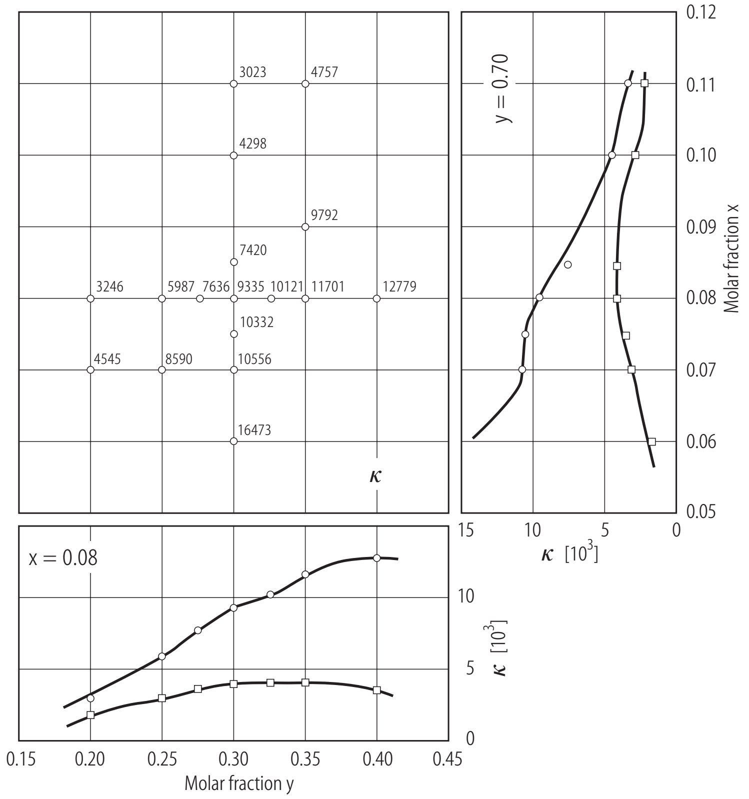

Fig. 1C-c66-029. $(Pb_{1-x}La_x)(Zr_{1-y}Ti_y)_{1-x/4}O_4$ (PLZT 100x/100y/100(1−y)) (ceramics). κ_{max}, κ_{RT} vs. x, y [91Ohk]. κ_{max}: maximum dielectric constant. κ_{RT}: dielectric constant at RT. f = 10 kHz. Circles: κ_{max}. Squares: κ_{RT}.

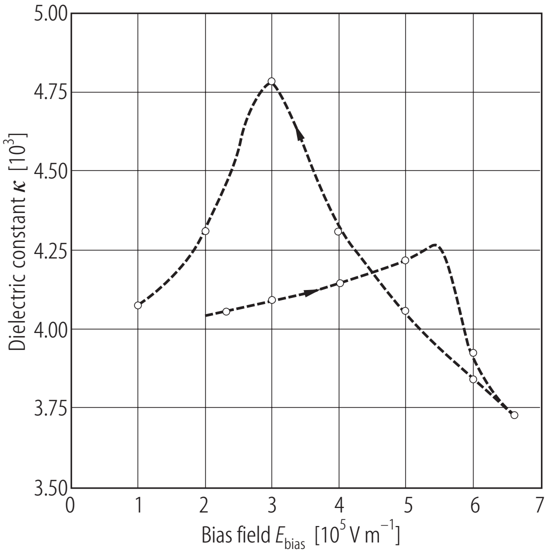

Fig. 1C-c66-030. $(Pb_{0.91}La_{0.09})(Zr_{0.65}Ti_{0.35})_{0.977}O_3$ (PLZT 9/65/35) (ceramics). κ vs. E_{bias} [92Bot]. T = RT. f = 180 kHz.

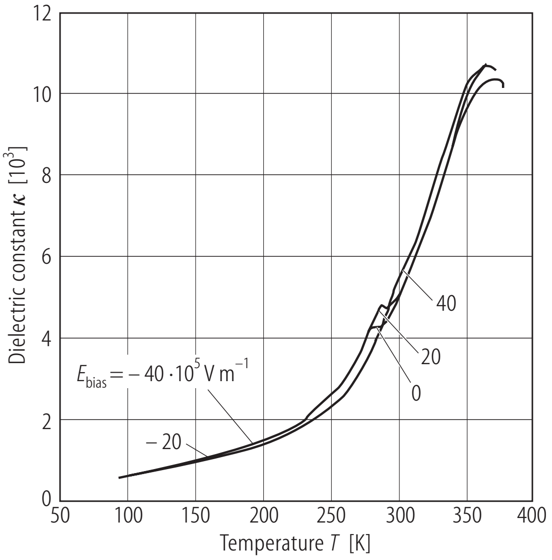

Fig. 1C-c66-031. $(Pb_{0.91}La_{0.09})(Zr_{0.65}Ti_{0.35})_{0.977}O_3$ (PLZT 9/65/35) (ceramics). κ vs. T [92Bot]. Parameter: E_{bias}. f = 180 kHz.

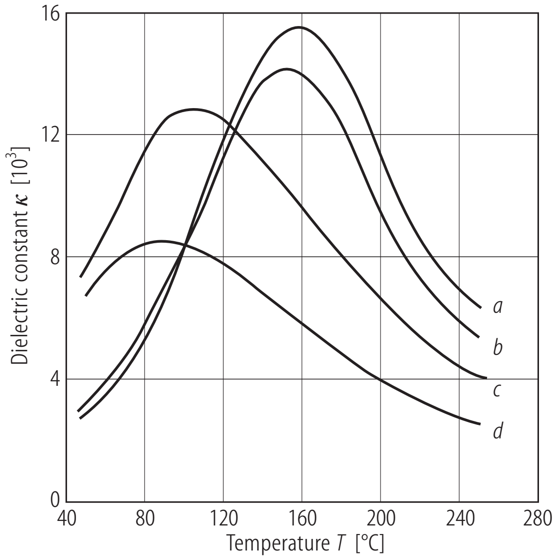

Fig. 1C-c66-032. $(Pb_{1-x}La_x)(Zr_{0.65}Ti_{0.35})_{1-x/4}O_3$ (PLZT 100x/65/35) (ceramics). κ vs. T [89Mig]. Parameter: x. f = 126 kHz. Curve *a*: x = 0.07; *b*: x = 0.08; *c*: x = 0.09; *d*: x = 0.10.

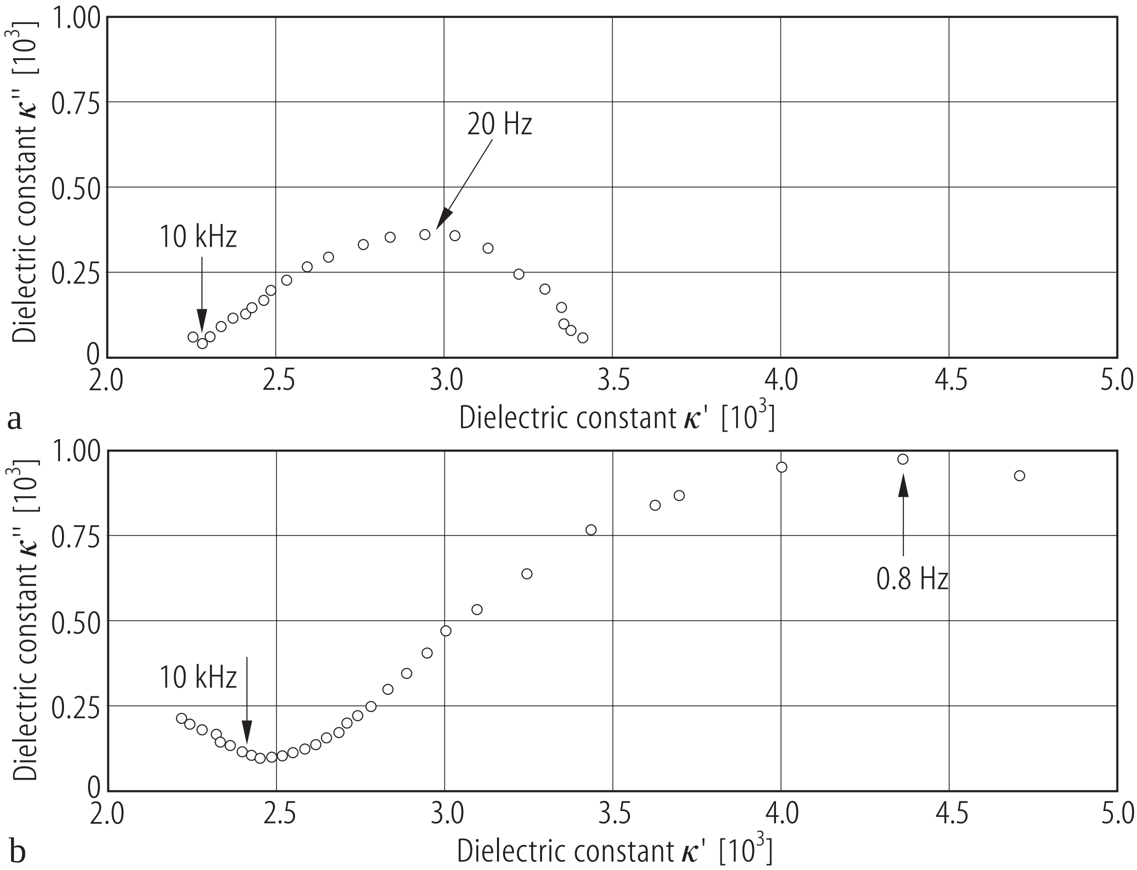

Fig. 1C-c66-033. $(Pb_{0.91}La_{0.09})(Zr_{0.65}Ti_{0.35})_{0.98}O_3$ (PLZT 9/65/35) (ceramics). *κ*' vs. *κ*'' [94Del]. **(a)** T = 480 K. **(b)** T = 435 K.

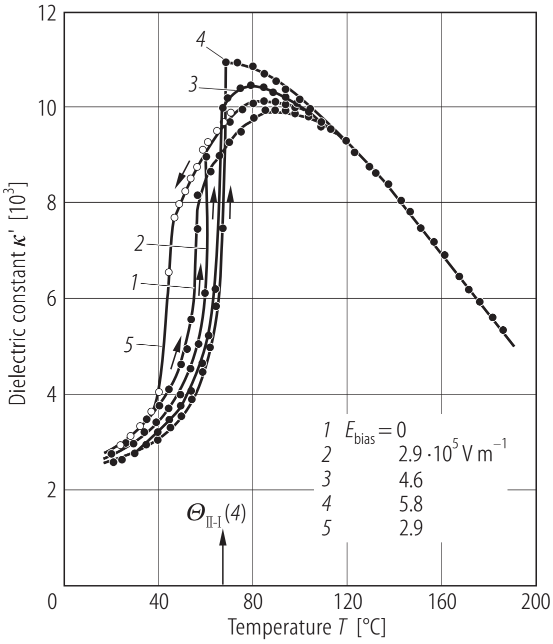

Fig. 1C-c66-034. $(Pb_{0.90}La_{0.10})(Zr_{0.55}Ti_{0.45})_{0.98}O_3$ (PLZT 10/55/45) (ceramics). κ' vs. T [86Yok]. Parameter: E_{bias}.

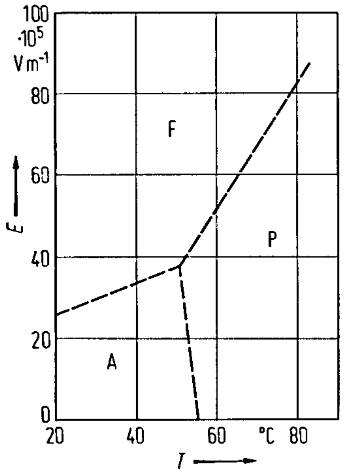

Fig. 1C-c66-035. PLZT(11.1/55/45). *E*−*T* phase diagram [76Wol].

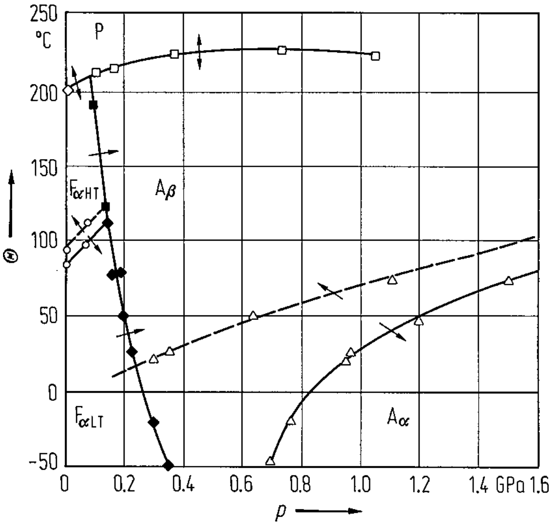

Fig. 1C-c66-036. $(Pb_{0.98}La_{0.02})(Zr_{0.92}Ti_{0.08})O_3$ (ceramics). Θ vs. p [78Fri]. p: hydrostatic pressure. Arrows indicate the directions of pressure or temperature change, i.e. solid lines indicate boundary at increasing pressure, dashed line indicates the reverse transformation.

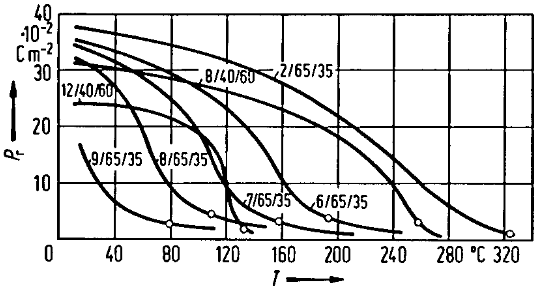

Fig. 1C-c66-037. PLZT. P_r vs. T [71Hae2]. Parameter: composition. P_r: remanent polarization.

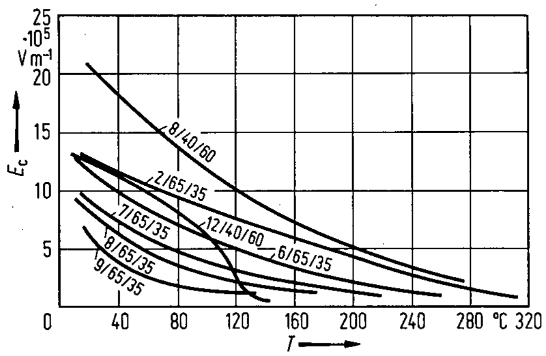

Fig. 1C-c66-038. PLZT. E_c vs. T [71Hae2]. Parameter: composition.

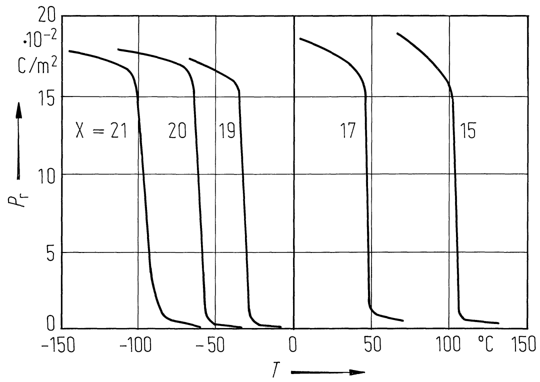

Fig. 1C-c66-039. PLZT(X/30/70) (ceramics). P_r vs. T [80Ste2]. Parameter: X. P_r: remanent polarization.

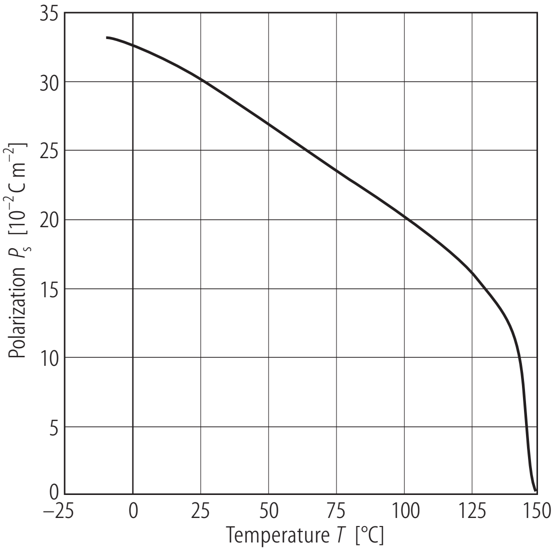

Fig. 1C-c66-040. $(Pb_{0.92}La_{0.08})(Zr_{0.40}Ti_{0.60})_{0.98}O_3$ (PLZT 8/40/60) (ceramics). P_s vs. T [87Deb].

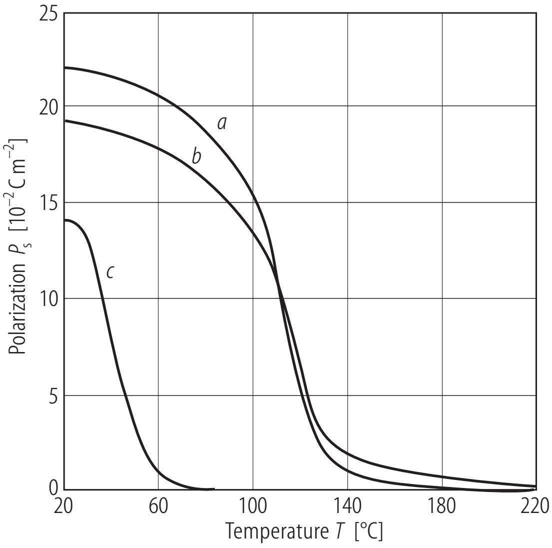

Fig. 1C-c66-041. $(Pb_{1-x}La_x)(Zr_{0.65}Ti_{0.35})_{1-x/4}O_3$ (PLZT 100x/65/35) (ceramics). P_s vs. T [89Mig]. Parameter: x. Curve *a*: x = 0.07, *b*: x = 0.08, *c*: x = 0.09. The samples were poled at 22 °C.

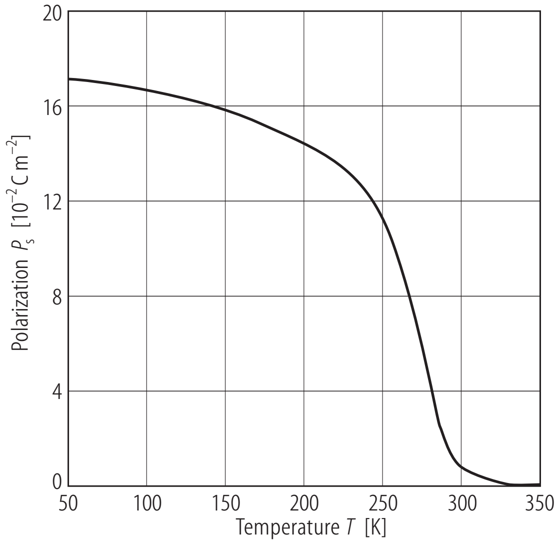

Fig. 1C-c66-042. $(Pb_{0.91}La_{0.09})(Zr_{0.65}Ti_{0.35})_{0.977}O_3$ (PLZT 9/65/35) (ceramics). P_s vs. T [92Bot].

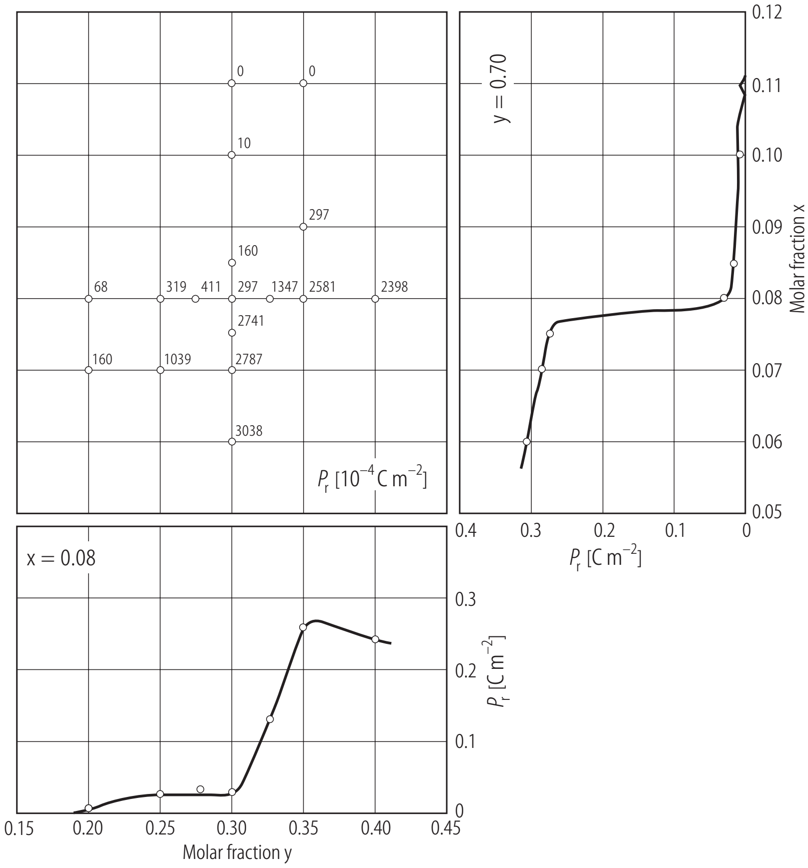

Fig. 1C-c66-043. $(Pb_{1-x}La_x)(Zr_{1-y}Ti_y)_{1-x/4}O_3$ (PLZT) (ceramics). P_r vs. x, y [91Ohk].

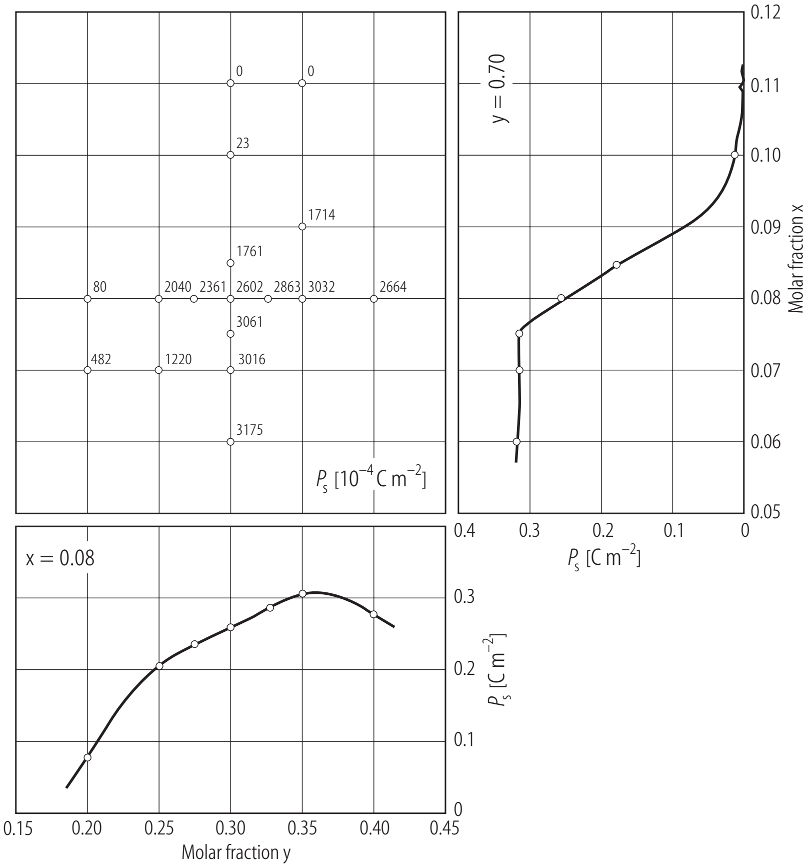

Fig. 1C-c66-044. $(Pb_{1-x}La_x)(Zr_{1-y}Ti_y)_{1-x/4}O_3$ (PLZT) (ceramics). P_s vs. x, y [91Ohk].

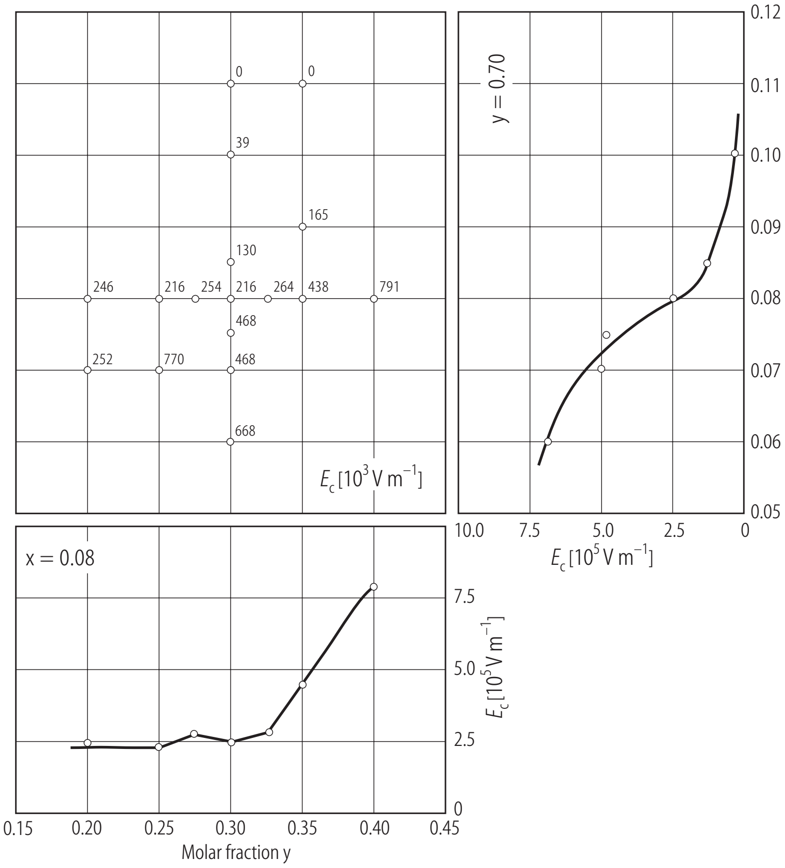

Fig. 1C-c66-045. $(Pb_{1-x}La_y)(Zr_{1-y}Ti_y)_{1-x/4}O_3$ (PLZT) (ceramics). E_c vs. x, y [91Ohk].

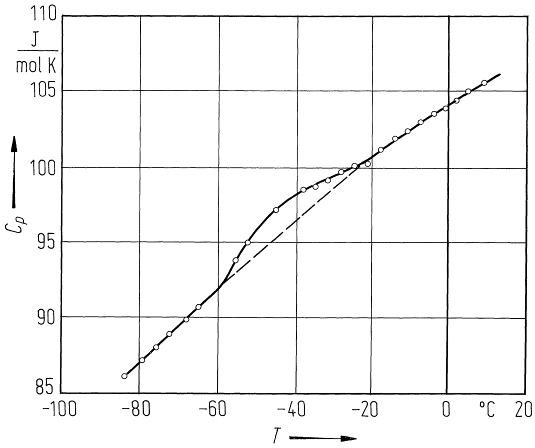

Fig. 1C-c66-046. PLZT(20/30/70) (ceramics). C_p vs. T [80Ste3].

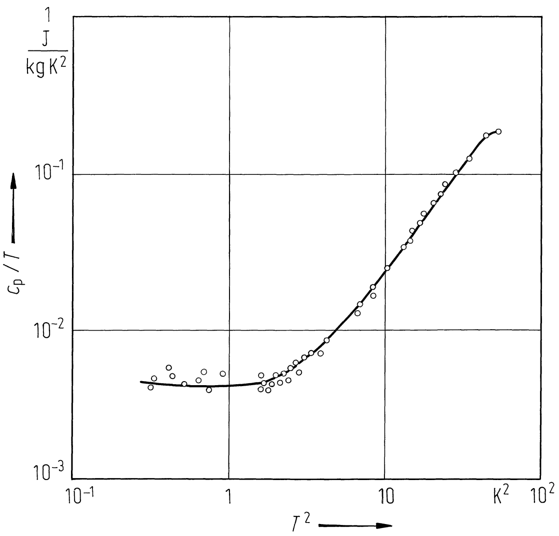

Fig. 1C-c66-047. PLZT(10/65/35) (ceramics). c_p/T vs. T^2 [82Hen].

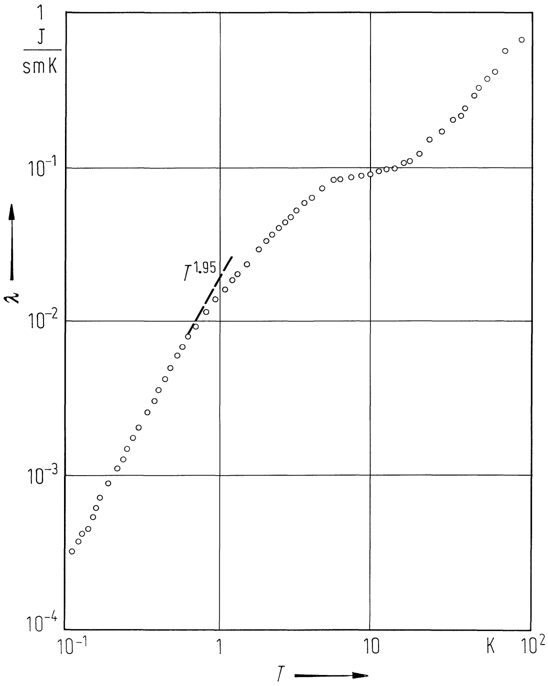

Fig. 1C-c66-048. PLZT(8.5/65/35) (ceramics). λ vs. T [81Fis]. λ: thermal conductivity.

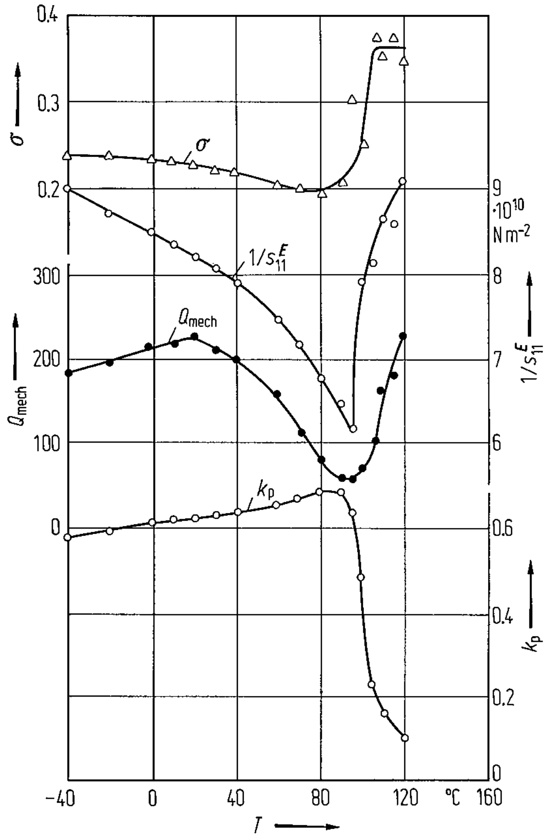

Fig. 1C-c66-049. PLZT(7.2/65/35). $1/s_{11}^E$, k_p, σ and Q_{mech} vs. T [73Mei]. σ: Poisson's ratio.

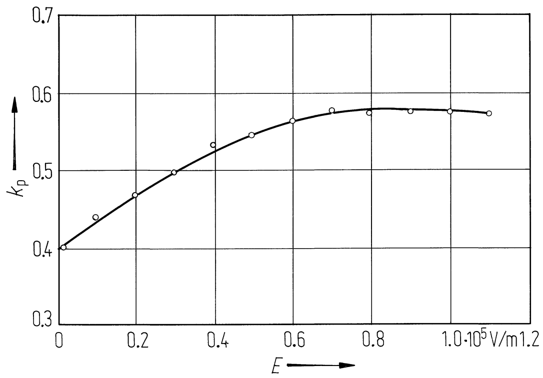

Fig. 1C-c66-050. $(Pb_{0.98}La_{0.02})(Fe_{0.02}Zr_{0.51}Ti_{0.47})O_3$ (ceramics). k_p vs. E [83Jem].

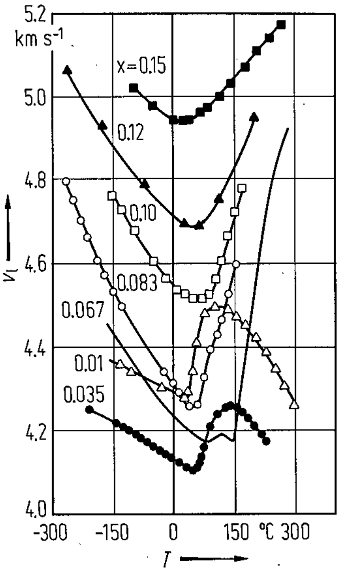

Fig. 1C-c66-051. $(Pb_{1.02-x}La_x)(Zr_{0.65}Ti_{0.35})O_3$ (unpoled ceramics). v_l vs. T [72Kra]. Parameter: x. v_l: ultrasonic longitudinal velocity. (Compositions indicated seem a little ambiguous.)

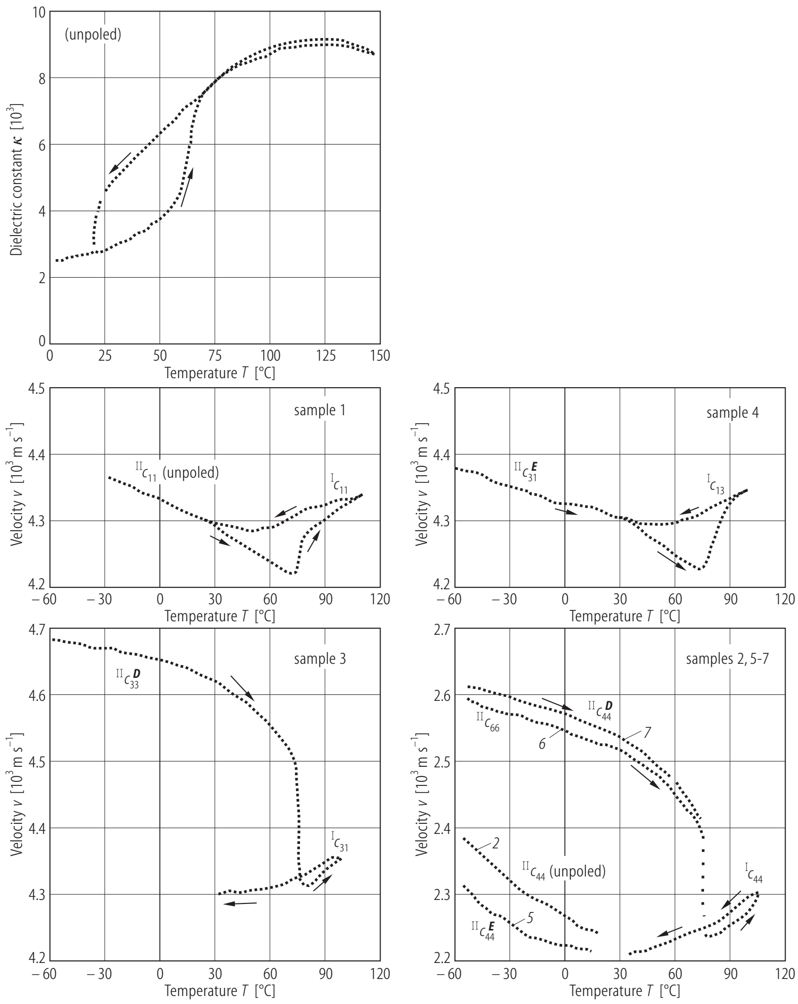

Fig. 1C-c66-052. PLZT(9.8/55/45). *κ*, *υ* vs. *T* [87Sak]. *κ*: dielectric constant, *υ*: ultrasonic sound velocity. Measuring conditions of each sample are as follows:

Sample No.	Mode of propagation	Poling	Corresponding elastic stiffness constants
1	L	none	$^{II}c_{11}$ (unpoled), $^{I}c_{11}$
2	T	none	$^{II}c_{44}$ (unpoled), $^{I}c_{44}$
3	L: $\boldsymbol{k} \parallel 3$	$P_s \parallel 3$	$^{II}c_{33}^{\boldsymbol{D}}$, $^{I}c_{31}$
4	L: $\boldsymbol{k} \perp 3$	$P_s \parallel 3$	$^{II}c_{13}^{\boldsymbol{E}}$, $^{I}c_{31}$
5	T: $\boldsymbol{k} \parallel 3$, $u \parallel 2$	$P_s \parallel 3$	$^{II}c_{44}^{\boldsymbol{E}}$, $^{I}c_{44}$
6	T: $\boldsymbol{k} \parallel 1$, $u \parallel 2$	$P_s \parallel 3$	$^{II}c_{66}$, $^{I}c_{44}$
7	T: $\boldsymbol{k} \parallel 2$, $u \parallel 3$	$P_s \parallel 3$	$^{II}c_{44}^{\boldsymbol{D}}$, $^{I}c_{44}$

L: longitudinal, T: transversal, ***k*** **:** wave vector, *u*: particle displacement, c^E and c^D: stiffness constants measured at constant *E* and *D*, respectively. Superscripts I and II stand for high temperature paraelectric phase and low temperature ferroelectric phase, respectively. *f* = 10 MHz for longitudinal wave and 2.3 MHz for transverse wave.

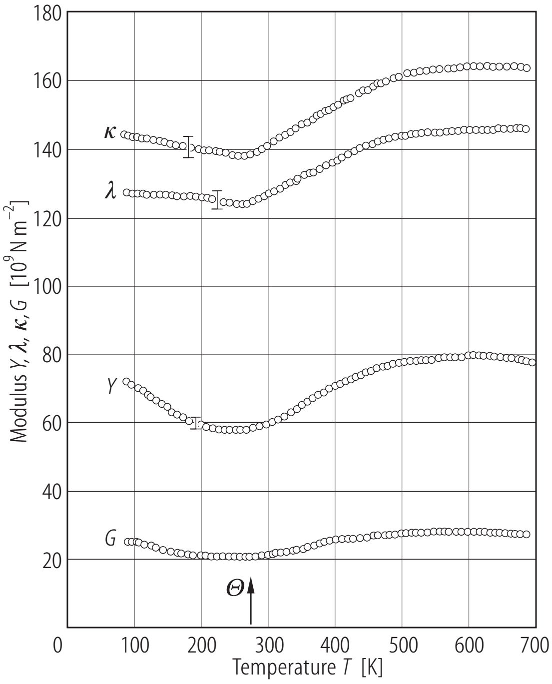

Fig. 1C-c66-053. PLZT(20/30/70). Elastic constants vs. *T* [89Yus]. *Y*: Young's modulus, λ: Lame's modulus, κ: bulk modulus, *G*: shear modulus.

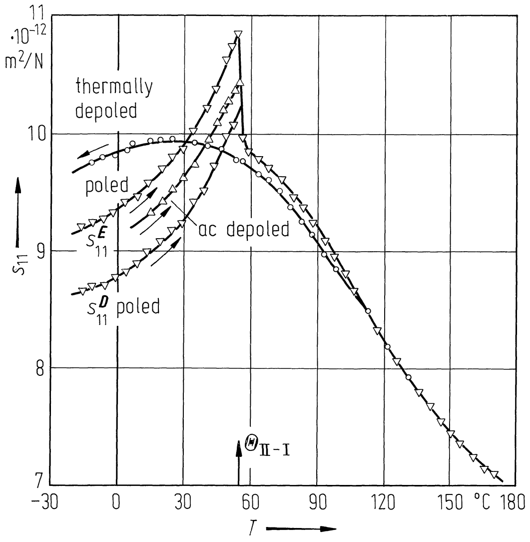

Fig. 1C-c66-054. PLZT(10/55/45) (ceramics). s_{11} vs. T [86Yok]. s_{11}: elastic compliance.

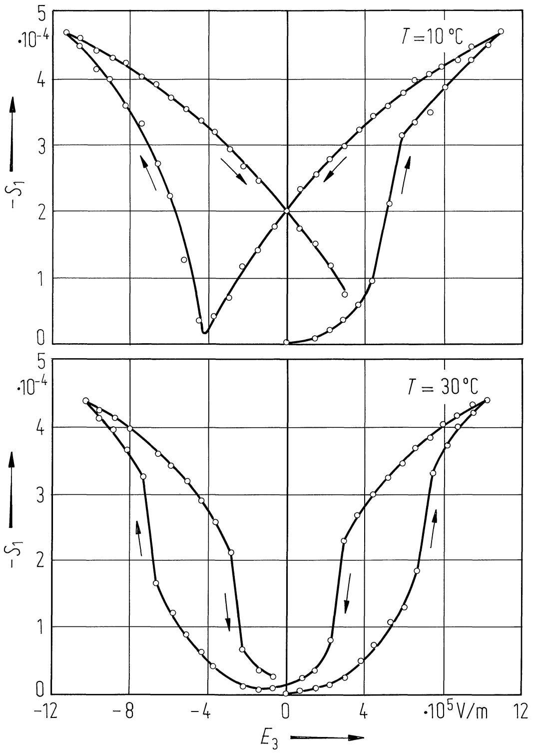

Fig. 1C-c66-055. PLZT(11/55/45) (ceramics). S_1 vs. E_3 [86Yok]. S_1: component of strain tensor. $S_1 \perp E_3$.

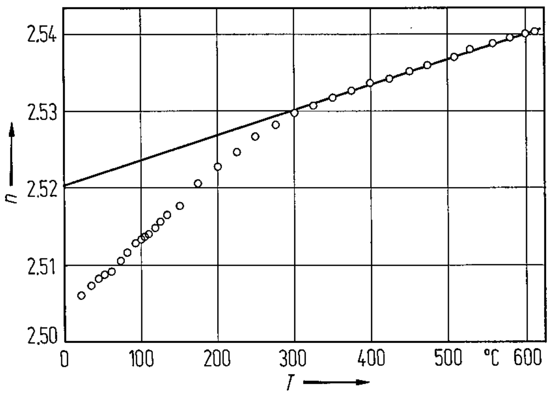

Fig. 1C-c66-056. PLZT(8/65/35). *n* vs. *T* [73Bur]. λ = 633 nm.

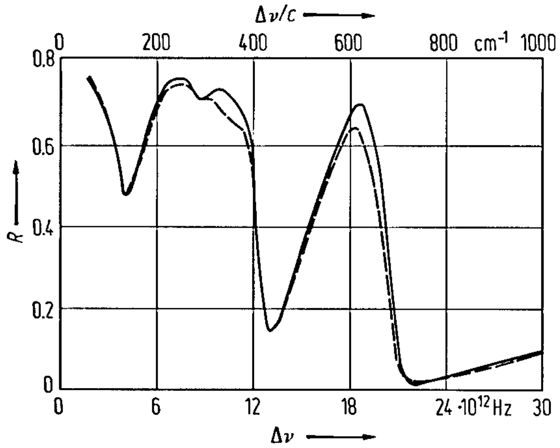

Fig. 1C-c66-057. PLZT(12/40/60). *R* vs. Δ*ν* [74Lur]. *R*: infrared reflectivity at RT (solid curve) and 200 °C (dashed curve).

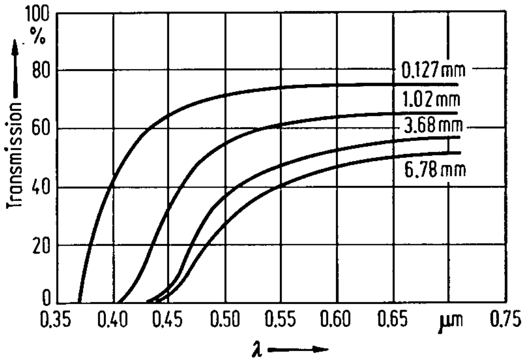

Fig. 1C-c66-058. PLZT(9/65/35). Transmission vs. λ [71Hae2]. Parameter: thickness.

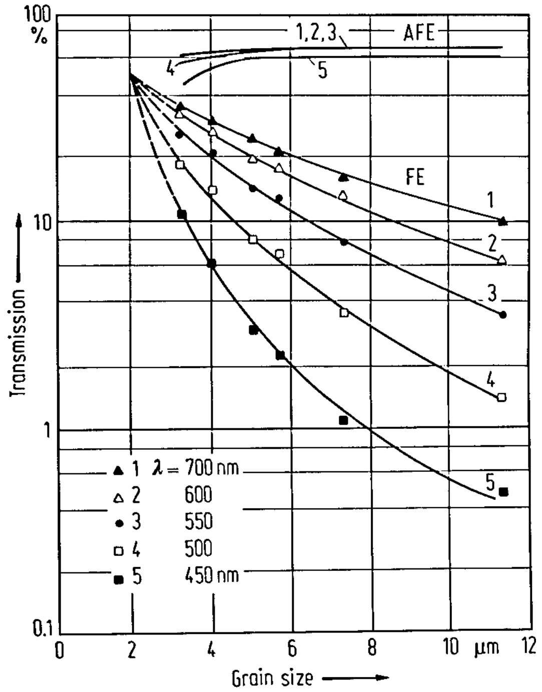

Fig. 1C-c66-059. PLZT(7.6/70/30). Transmission vs. grain size [75Mat]. Parameter: λ. AFE: originally antiferroelectric phase, FE: field-induced ferroelectric phase. Detector aperture: 30'.

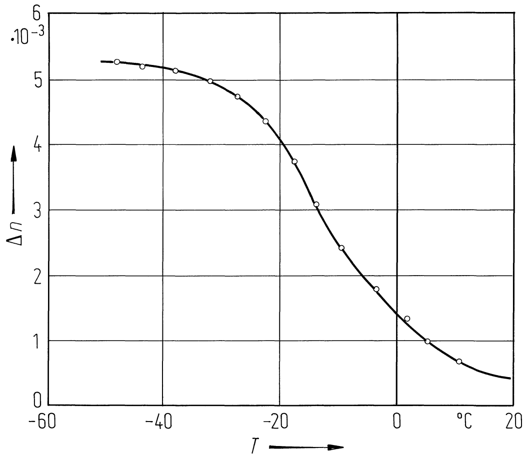

Fig. 1C-c66-060. PLZT(10/65/35) (ceramics). Δ*n* vs. *T* [84Cor].

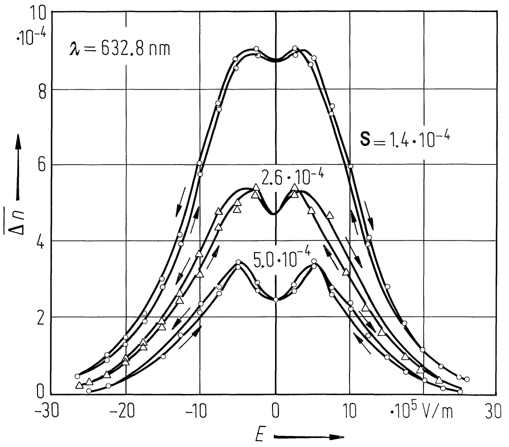

Fig. 1C-c66-061. PLZT(9/65/35) (ceramics). $\overline{\Delta n}$ vs. E [80Fog]. Parameter: strain **S**. $\overline{\Delta n}$: effective birefringence.

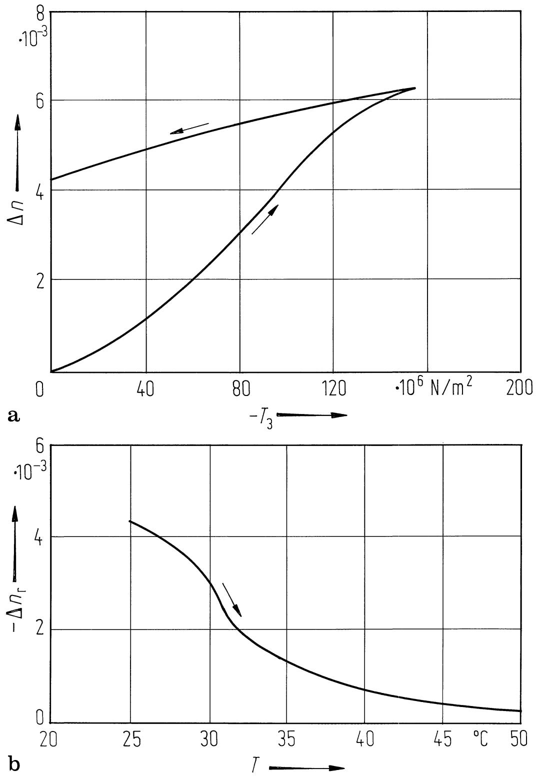

Fig. 1C-c66-062. PLZT(8/65/35) (ceramics). **(a)** Δn vs. $-T_3$, **(b)** Δn_r vs. T [84Arn]. Δn_r: remanent birefringence. T_3: component of stress tensor.

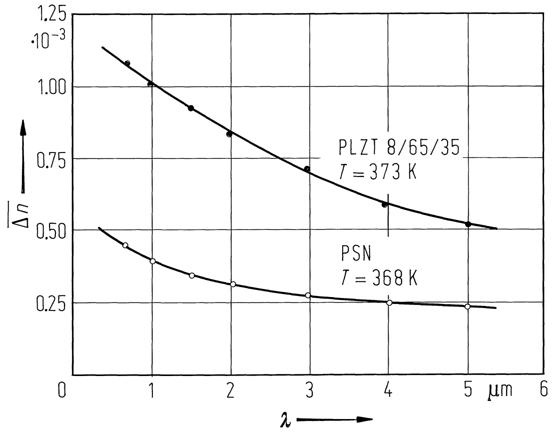

Fig. 1C-c66-063. $Pb(Sc_{1/2}Nb_{1/2})O_3$ (PSN), PLZT(8/65/35). $\overline{\Delta n}$ vs. λ [86Kni]. $\overline{\Delta n}$: effective birefringence under electric field. Length is 1.5 mm, electrode separation is 1.5 mm, $V = 1$ kV.

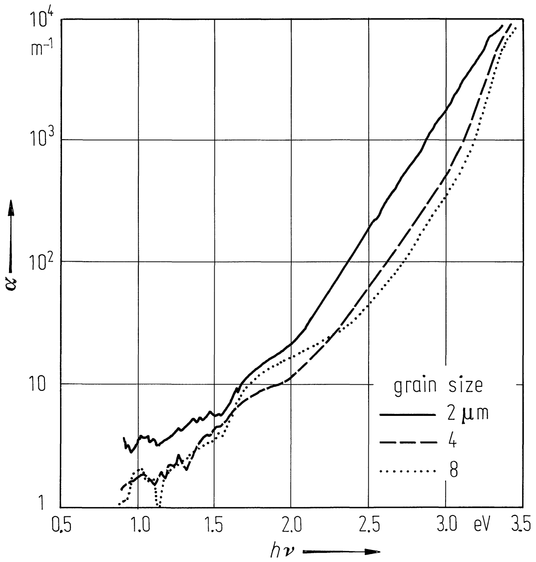

Fig. 1C-c66-064. PLZT(7/65/35) (ceramics). α vs. $h\nu$ [84Sea]. Parameter: grain size.

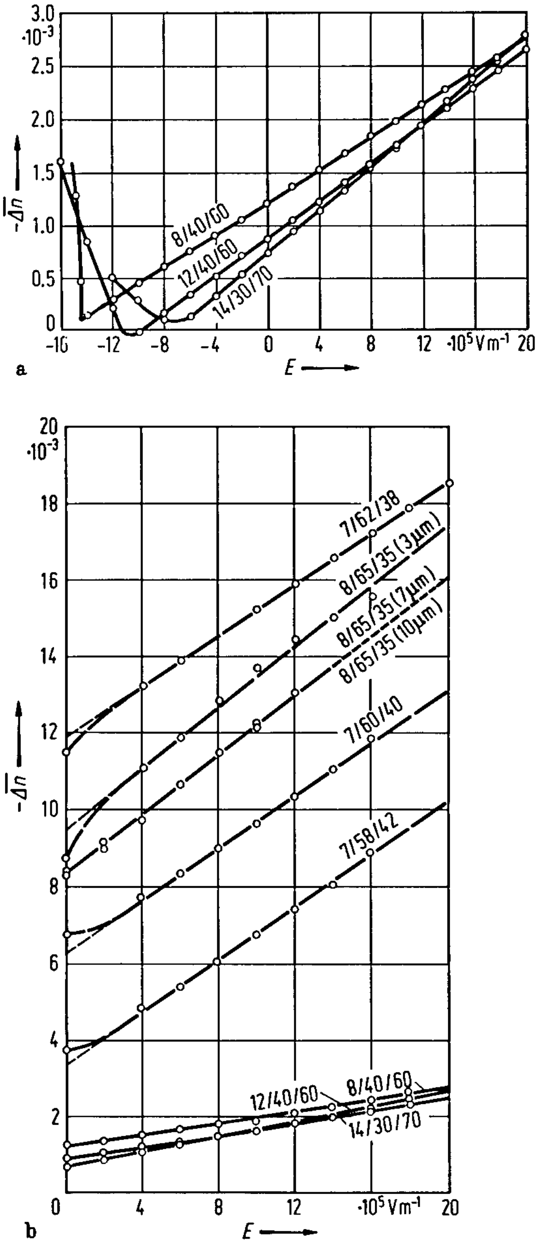

Fig. 1C-c66-065. PLZT. $\overline{\Delta n}$ vs. E [71Hae1]. Parameter: composition. $\overline{\Delta n}$: effective birefringence. λ = 633 nm.

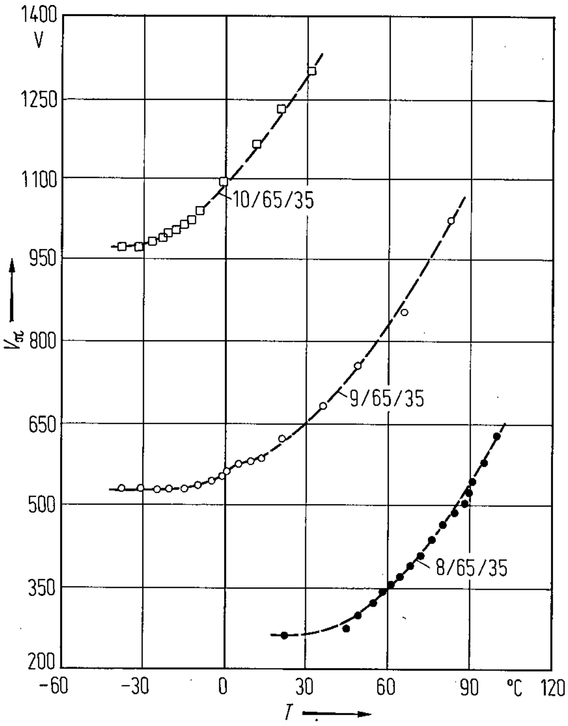

Fig. 1C-c66-066. PLZT (X/65/35). V_π vs. T [76Har]. Parameter: composition. V_π: half-wave voltage at λ = 500 nm. Electrode gap: 1 mm, thickness: 0.25 nm.

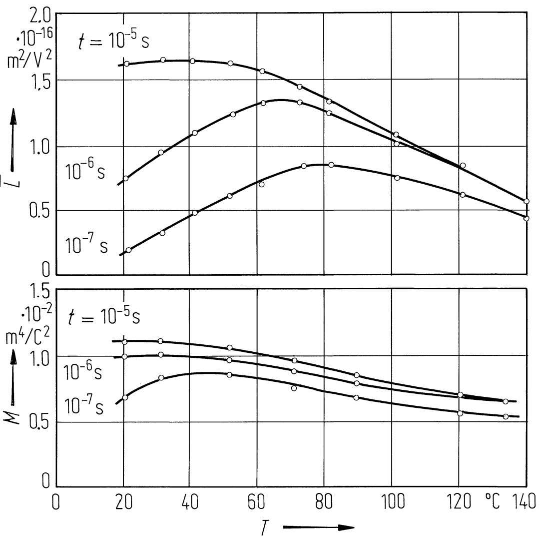

Fig. 1C-c66-067. PLZT(10/65/35) (ceramics). $\bar{L}$, $\bar{M}$ vs. T [82Ozo]. $\bar{L}$, $\bar{M}$: effective quadratic electrooptic constants, $\bar{L}$ for E, $\bar{M}$ for P. Parameter: t, time after the field application. λ = 632.8 nm.

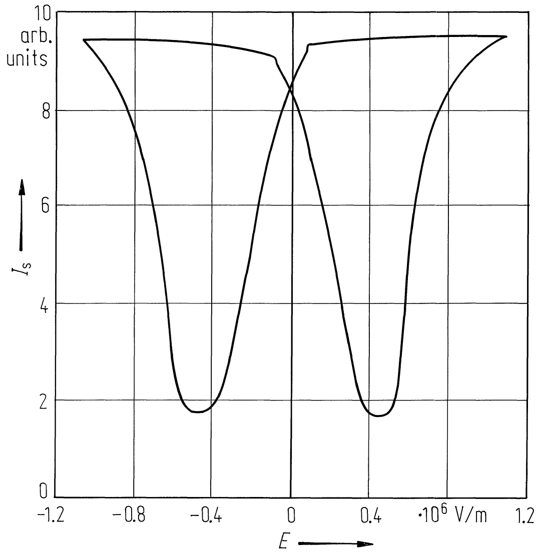

Fig. 1C-c66-068. PLZT(7/65/35) (ceramics). I_s vs. E [80Lan]. I_s: scattered light intensity when P_s is reversed.

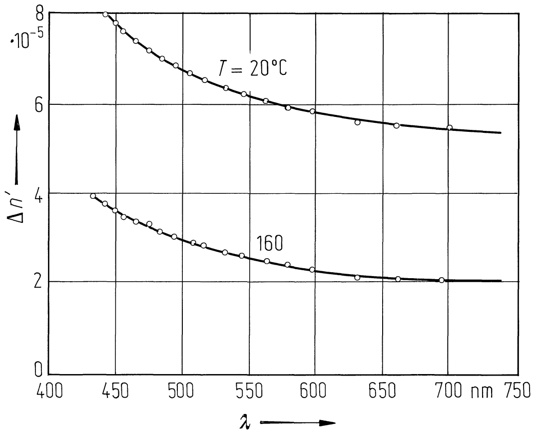

Fig. 1C-c66-069. PLZT(9/65/35) (ceramics). Δ*n*' vs. λ [80Ozo]. Δ*n*': stress-induced birefringence at uniaxial stress of $5 \cdot 10^6$ Nm^{-2}. Parameter: temperature.

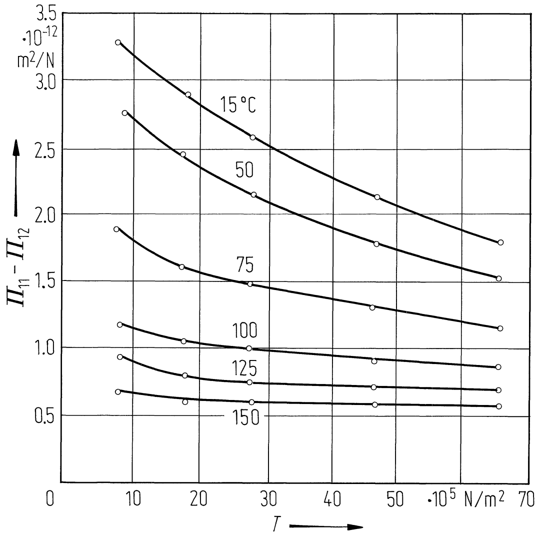

Fig. 1C-c66-070. PLZT(9/65/35) (ceramics). Π_{11}–Π_{12} vs. T [80Ozo]. Π_{11}, $-\Pi_{12}$: piezooptic constants for **T**, **T**: uniaxial stress. Parameter: temperature. λ = 632.8 nm.

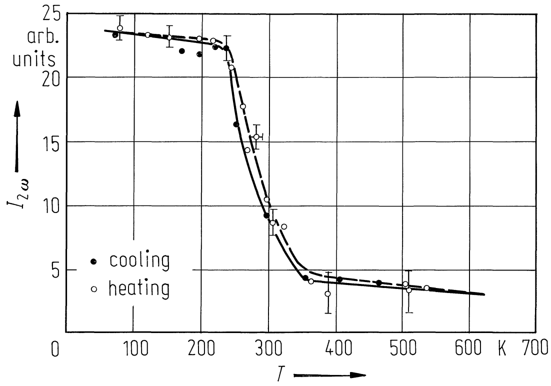

Fig. 1C-c66-071. PLZT(9/65/35) (ceramics). $I_{2\omega}$ vs. T [79Bet]. λ = 1.064 μm. $I_{2\omega}$: optical second harmonic intensity.

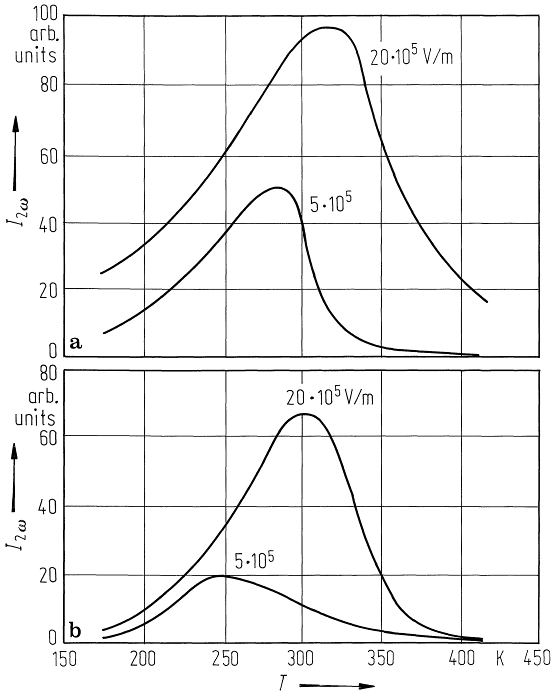

Fig. 1C-c66-072. PLZT(7.6/70/30) (ceramics) **(a)**, PLZT(8.3/70/30) (ceramics) **(b)**. $I_{2\omega}$ vs. T [86Kun]. λ = 1.06 µm. $I_{2\omega}$: optical second harmonic intensity under E_{bias}. Parameter: E_{bias}.

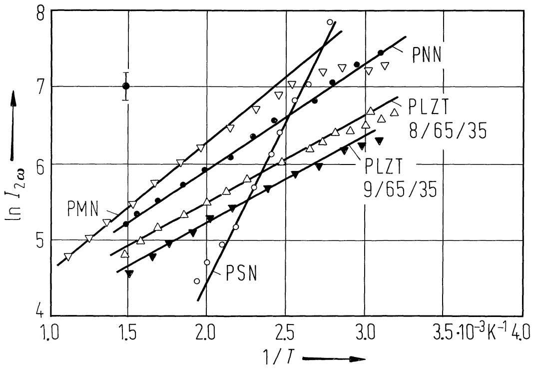

Fig. 1C-c66-073. $Pb(Sc_{1/2}Nb_{1/2})O_3$ (PSN), $Pb(Ni_{1/3}Nb_{2/3})O_3$ (PNN), $Pb(Mg_{1/3}Nb_{2/3})O_3$ (PMN), PLZT. $\ln I_{2\omega}$ vs. $1/T$ [81Lib]. $I_{2\omega}$: optical second harmonic intensity. λ = 1.064 µm. $I_{2\omega}$ in arbitrary units.

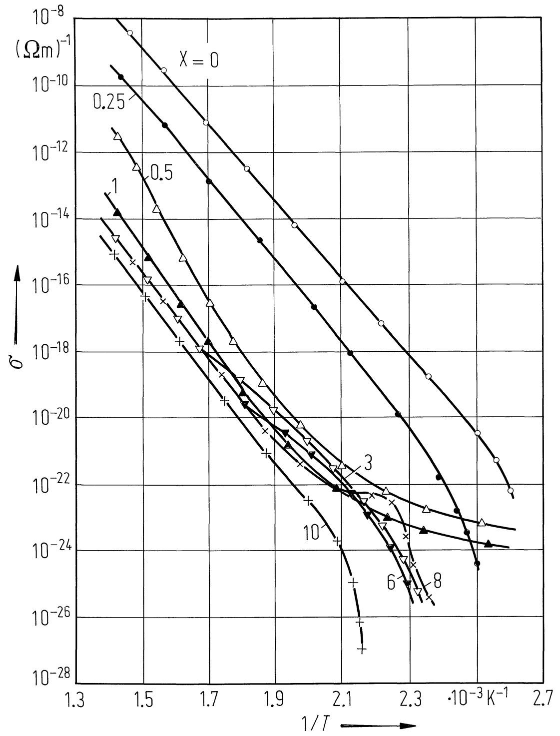

Fig. 1C-c66-074. PLZT(X/52/48) (ceramics). σ vs. $1/T$ [86Woj]. σ: dark conductivity. Parameter: X.

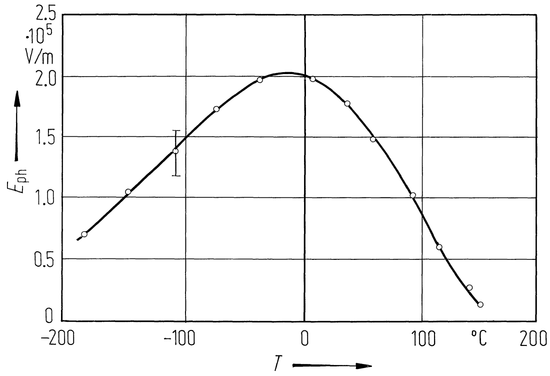

Fig. 1C-c66-075. PLZT(7/65/35) (ceramics). E_{ph} vs. T [85Kur]. E_{ph}: photovoltaic field.

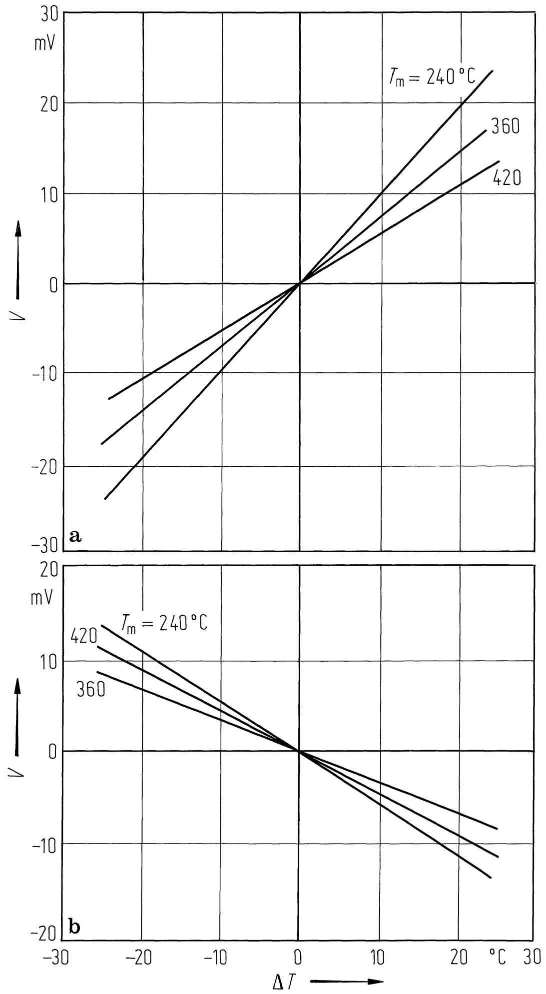

Fig. 1C-c66-076. PLZT (0.5/52/48) (ceramics) (**a**), PLZT (10/52/48) (ceramics) (**b**). *V* vs. Δ*T* for PLZT [86Woj]. *V*: thermoelectromotive force. Δ*T*: temperature difference. Parameter: T_m. T_m: mean temperature during the measurement.

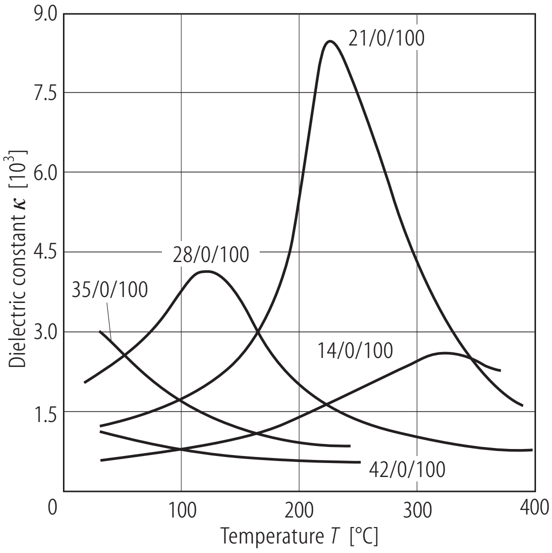

Fig. 1C-c66-077. $(Pb_{1-x}La_x)Ti_{1-x/4}O_3$ (PLZT 100x/0/100) (thin film). κ vs. T [83Ada]. Parameter: x. f = 100 kHz. Film thickness: 0.4 µm.

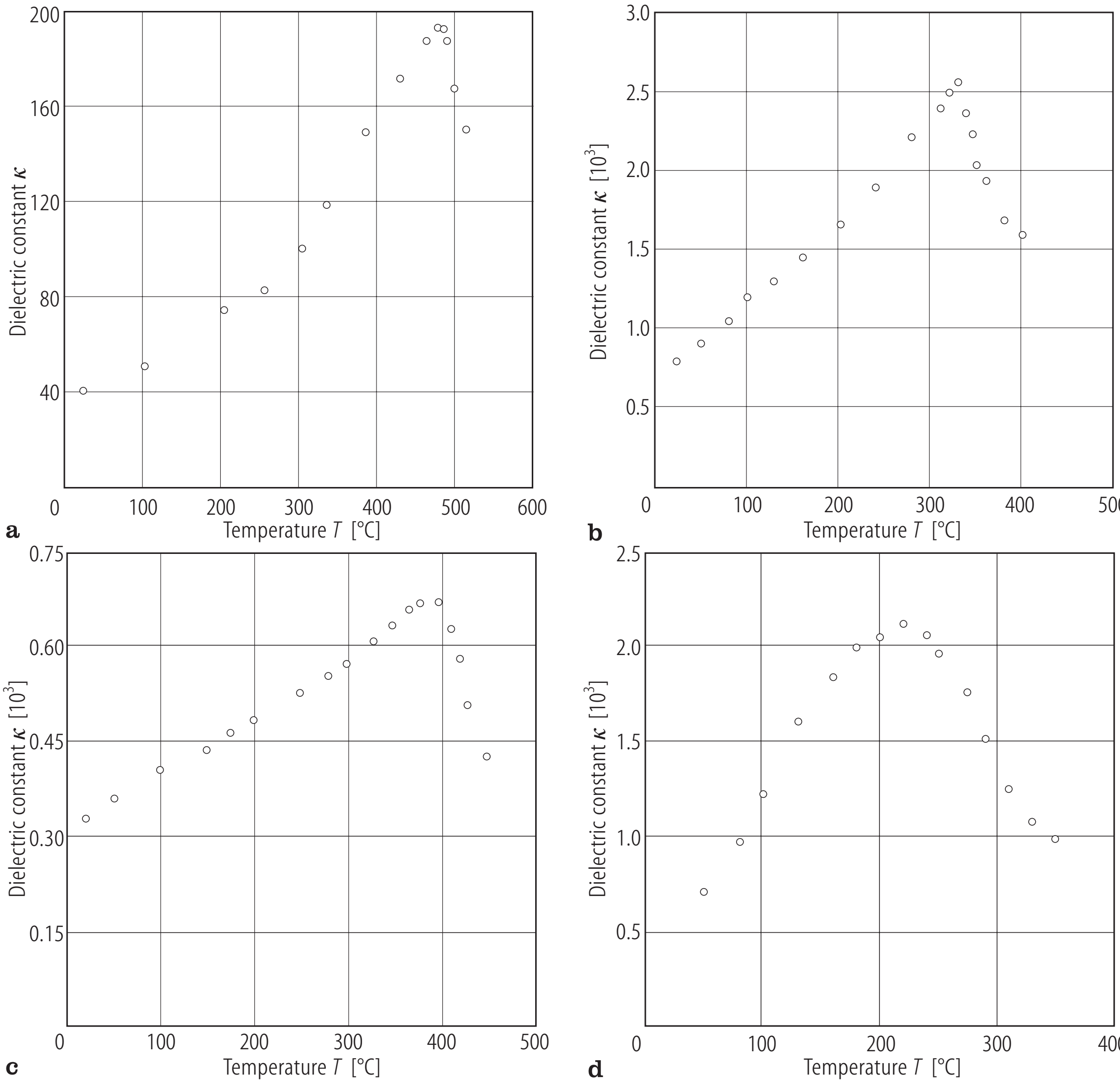

Fig. 1C-c66-078. $(Pb_{1-x}La_x)(Zr_{1-y}Ti_y)O_3$ (thin film). κ vs. T [94YeC]. f = 1 kHz. Film thickness: 4500...6000 Å. (**a**) x = 0, y = 1.0; (**b**) x = 0, y = 0.46; (**c**) x = 0.05, y = 1.0; (**d**) x = 0.09, y = 0.35.

References

71Bry Brya, W.J.: Phys. Rev. Lett. **26** (1971) 1114; erratum: **26** (1971) 1408.
71Hae1 Haertling, G.H., Land, C.E.: J. Am. Ceram. Soc. **54** (1971) 1.
71Hae2 Haertling, G.H.: J. Am. Ceram. Soc. **54** (1971) 303.
72Kra Krause, J.K., O'Bryan Jr., H.M.: J. Am. Ceram. Soc. **55** (1972) 497.
72Mei Meitzler, A.H., O'Bryan Jr., H.M.: J. Am. Ceram. Soc. **55** (1972) 504.
72Sin Singh, S., Remeika, J.P., Potopowicz, J.R.: Appl. Phys. Lett. **20** (1972) 291.
72Tha Thacher, P.D.: Ferroelectrics **3** (1972) 147.
73Cut Cutchen, J.T., Haertling, G.H.: J. Am. Ceram. Soc. **56** (1973) 225.
73Mei Meitzler, A.H., O'Bryan Jr., H.M.: Proc. IEEE **61** (1973) 959.
73Sno Snow, G.S.: J. Am. Ceram. Soc. **56** (1973) 479.
74Lan Land, C.E.: Ferroelectrics **7** (1974) 45.
74Liu Liu, S.T.: Ferroelectrics **7** (1974) 167.
74Luf Luff, D., Lane, R., Brown, K.R., Marshallsay, H.J.: Trans. J. Brit. Ceram. Soc. **73** (1974) 251.
74Lur Lurio, A., Burns, G.: J. Appl. Phys. **45** (1974) 1986.
74Wol Wolters, M., Burggraaf, A.J.: Phys. Status Solidi (a) **24** (1974) 341.
75Kev Keve, E.T., Bye, K.L.: J. Appl. Phys. **46** (1975) 810.
75Mat Matsuyama, I., Jyomura, S.: J. Am. Ceram. Soc. **58** (1975) 347.
75Wol Wolters, M., Burggraaf, A.J.: Mater. Res. Bull. **10** (1975) 417.
76Bye Bye, K.L.: Ferroelectrics **12** (1976) 221.
76Har Harris Jr., J.O., Cutchen, J.T.: Ferroelectrics **10** (1976) 175.
76Oka Okazaki, K., Ohtsubo, I., Toda, K.: Ferroelectrics **10** (1976) 195.
76Wol Wolters, M., Thieme, C.L.H., Burggraaf, A.J.: Mater. Res. Bull. **11** (1976) 315.
77Mat Matsui, Y., Higuma, Y., Okuyama, M., Nakagawa, T., Hamakawa, Y.: Proc. First Meeting on Ferroelectric Materials and Their Applications, Kyoto, Tanaka, T. (chairman), Kyoto: Department of Electronics, Kyoto University, 1977, p. 37.
77Miy Miyauchi, K., Toda, G.: Yogyo-Kyokaishi **85** (1977) 36.
77Tha Thacher, P.D.: Appl. Opt. **16** (1977) 3210.
77Yok Yokosuka, M.: Jpn. J. Appl. Phys. **16** (1977) 379.
78Fri Fritz, I.J., Keck, J.D.: J. Phys. Chem. Solids **39** (1978) 1163.
78Hig Higuma, Y., Matsui, Y., Okuyama, M., Nakagawa, T., Hamakawa, Y.: Jpn. J. Appl. Phys. **17**, Suppl. 17-1 (1978) 209.
78Mat Matsunami, H., Ishida, M., Tanaka, T.: J. Electron. Mater. **7** (1978) 229.
79Bet Betzler, K., Bauerle, D.: Appl. Phys. **18** (1979) 271.
79Lan Land, C.E.: IEEE Trans. Electron. Devices ED-**26** (1979) 1143.
79Nak Nakagawa, T., Yamaguchi, J., Usuki, T., Matsui, Y., Okuyama, M., Hamakawa, Y.: Jpn. J. Appl. Phys. **18** (1979) 897.
80Fog Fogel, Y., Bar-Chaim, N., Seidman, A.: Appl. Opt. **19** (1980) 1609.
80Fri Fritsberg, P.A., Shternberg, A.R., Fritsberg, V.Ya.: Izv. Akad. Nauk SSSR, Neorg. Mater. **16** (1980) 1234; Inorg. Mater. (English Transl.) **16** (1980) 852.
80Gur Gururaja, T.R., Subbarao, E.C.: Ferroelectrics **23** (1980) 101.
80Mat Matsunami, H., Kimura, K., Ishida, M., Tanaka, T.: J. Phys. Soc. Jpn. **49**, Suppl. B (1980) 194.
80Oku Okuyama, M., Usuki, T., Hamakawa, Y., Nakagawa, T.: Appl. Phys. **21** (1980) 339.
80Ozo Ozolinsh, M.P.: Phys. Status Solidi (a) **57** (1980) K123.
80Ste1 Stenger, C.G.F., Burggraaf, A.J.: J. Phys. Chem. Solids **41** (1980) 17.
80Ste2 Stenger, C.G.F., Burggraaf, A.J.: J. Phys. Chem. Solids **41** (1980) 31.
80Ste3 Stenger, C.G.F., Burggraaf, A.J.: J. Phys. Chem. Solids **41** (1980) 25.

81Fis Fischer, E., Hässler, W., Hegenbarth, E., Fritsberg,V.I.: Phys. Status Solidi (a) **66** (1981) K169.
81Gal Galkin, A.A., Ishchuk, V.M., Morozov, E.M.: Fiz. Tverd. Tela **23** (1981) 161; Sov. Phys. Solid State (English Transl.) **23** (1981) 90.
81Har Härdtl, K.H.: J. Am. Ceram. Soc. **64** (1981) 283.
81Kir Kirkby, C.J.: Ferroelectrics **37** (1981) 567.
81Lib Liberts, G.V., Fritsberg, V.Ya.: Phys. Status Solidi (a) **67** (1981) K81.
81Sch Schmidt, N.A.: Ferroelectrics **31** (1981) 105.
81Ste Sternberg, A., Hlidek, P., Zvára, M.: Phys. Status Solidi (a) **64** (1981) K149.
82Hen Henning, I., Frach, P., Hegenbarth, E., Fritsberg, V.I.: Phys. Status Solidi (a) **70** (1982) K7.
82Lan Land, C.E., Peercy, P.S.: Ferroelectrics **45** (1982) 25.
82Ozo Ozolinsh, M.: Mater. Res. Bull. **17** (1982) 741.
82Spr Sprogis, A., Dimza, V.: Phys. Status Solidi (a) **72** (1982) K57.
83Ada Adachi, H., Kawaguchi, T., Kitabatake, M., Wasa, T.: Jpn. J. Appl. Phys. **22**, Suppl. 22-2 (1983) 11.
83Jem Jemna, I., Luca, E., Nicolau, P., Tanasoiu, C., Ioan, C.: J. Am. Ceram. Soc. **66** (1983) C166.
83Ker Kersten, O., Rost, A., Schmidt, G.: Phys. Status Solidi (a) **75** (1983) 495.
83Lan Land, C.E., Peercy, P.S.: Ferroelectrics **50** (1983) 85.
83Ste Stenberg, A., Zvára, M., Hlidek, P.: Phys. Status Solidi (a) **75** (1983) K179.
83Yao Yao, X., Chen, Z.-L., Cross, L.E.: J. Appl. Phys. **54** (1983) 3399.
84Arn Arndt, H., Schmidt, G., Vogel, N.: Ferroelectrics **61** (1984) 9.
84Cor Corullon, A., Jimenez, B.: Ferroelectrics **54** (1984) 167.
84Ish Ishchuk, V.M., Zavadskii, É.A., Presnyakova, O.V.: Fiz. Tverd. Tela **26** (1984) 724; Sov. Phys. Solid State (English Transl.) **26** (1984) 437.
84Sea Seager, C.H., Land, C.E.: Appl. Phys. Lett. **45** (1984) 395.
85Kur Kurmins, A.E., Dimza, V.I., Seglins, J.A., Sprogis, A.A.: Ferroelectrics **63** (1985) 253.
85Lan Land, C.E.: Jpn. J. Appl. Phys. **24**, Suppl. 24-2 (1985) 134.
85Men Meng, Z.Y., Kumar, U., Cross, L.E.: J. Am. Ceram. Soc. **68** (1985) 459.
85Smi Smits, J.G.: Ferroelectrics **64** (1985) 275.
85Uch Uchino, K., Aizawa, M.: Jpn. J. Appl. Phys. **24**, Suppl. 24-3 (1985) 139.
86Kni Knite, M., Sternberg, A., Ozolinsh, M.: Ferroelectrics **69** (1986) 89.
86Kun Kundzinsh, M., Liberts, G.: Ferroelectrics **69** (1986) 75.
86Woj Wójcik, K., Blaszczak, J., Handerek, J.: Ferroelectrics **70** (1986) 39.
86Yok Yokosuka, M., Marutake, M.: Jpn. J. Appl. Phys. **25** (1986) 981.
87Deb Deb, K.K.: Mater. Lett. **5** (1987) 222.
87Nag Nagata, K., Okazaki, K., Nanba, N., Honma, T.: Jpn. J. Appl. Phys. **26**, Suppl. 26-2 (1987) 129.
87Sas Sasaki, Y., Yokosuka, M., Marutake, M.: Jpn. J. Appl. Phys. **26**, Suppl. 26-2 (1987) 136.
89Mig Miga, S., Wójcik, K.: Ferroelectrics **100** (1989) 167.
89Yus Yushin, N.K., Bazarova, L.F., Gulyamov, G.: Ferroelectrics **90** (1989) 57.
90Boy Boyer, L.L., Wu, A.Y., McNeil, J.R.: Mater. Res. Soc. Symp. Proc. **200** (1990) 97.
90Nag Nagata, K., Nanba, N.: Ferroelectrics **109** (1990) 241.
90Pet Petersen, G.A., Zou, L.C., Van Buren, W.M., Boyer, L.L.: Mater. Res. Soc. Symp. Proc. **200** (1990) 127.
91Ohk Ohkubo, S., Suzuki, R., Segawa, H., Suzuki, T.: Ceramic Today-Tomorrow's Ceramics, Vicenzini, P. (ed.), Elsevier Science, 1991, p. 2379.
91Sug Sugiyama, S., Takagi, A., Tsuzuki, K.: Jpn. J. Appl. Phys. **30** (1991) 2170.
92Bot Böttger, U., Biermann, A., Arlt, G.: Ferroelectrics **134** (1992) 253.
92Oka Okada, M., Tominaga, K.: J. Appl. Phys. **71** (1992) 1955.
92Pet Petersen, G.A., McNeil Jr, J.R.: Thin Solid Films **220** (1992) 87.
92Pla Plaude, A.: Ferroelectrics **131** (1992) 257.
92Tos Tossel, D.A., Shorrocks, N.M., Obhi, J.S., Whatmore, R.W.: Ferroelectrics **134** (1992) 297.

93Dai Dai, X., DiGiovanni, A., Viehland, D.: J. Appl. Phys. **74** (1993) 3399.
93DeG DeGraef, M., Clark, D.R., Speck, J.S.: Ultramicroscopy **52** (1993) 179.
93Tom Tominaga, K., Shirayanagi, K., Takagi, T., Okada, M.: Jpn. J. Appl. Phys. **32** (1993) 4082.
94Del Dellis, J.-L., Dallennes, J., Carpentier, J.-L., Morell, A., Farhi, R.: J. Phys. Condens. Matter **6** (1994) 5161.
94Tom Tominaga, K., Sakashita, T., Nakashima, H., Okada, M.: J. Cryst. Growth **145** (1994) 219.
94YeC Ye, C., Baude, P., Polla, D.: Ferroelectrics **157** (1994) 347.
94Zha Zhang, X., Joy, D.C., Allard, L.F., Nolan, T.A.: Ferroelectrics **157** (1994) 159.